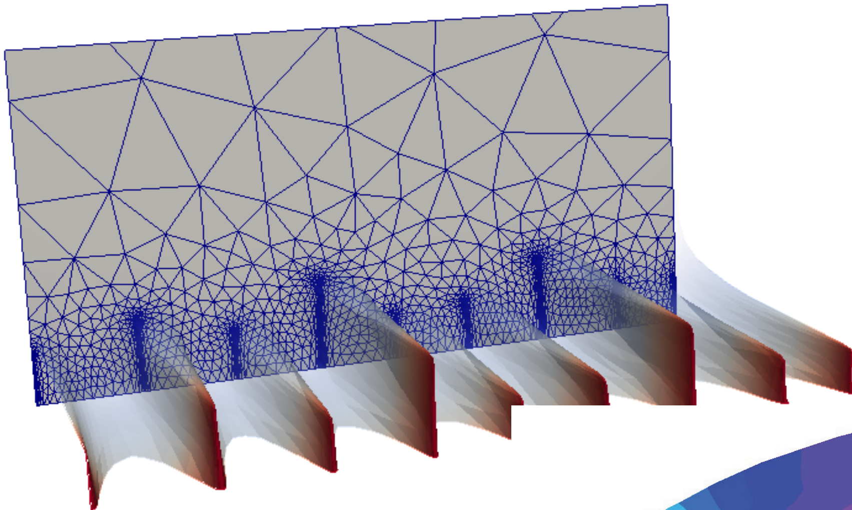

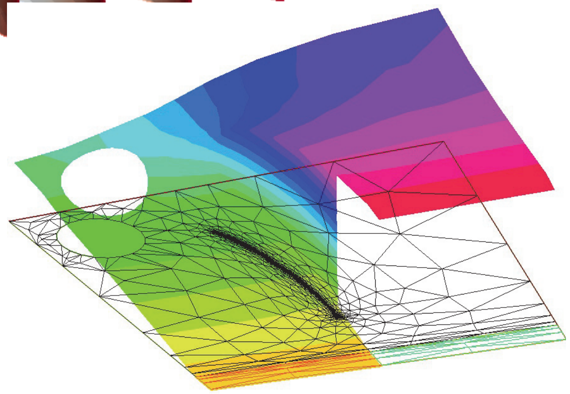

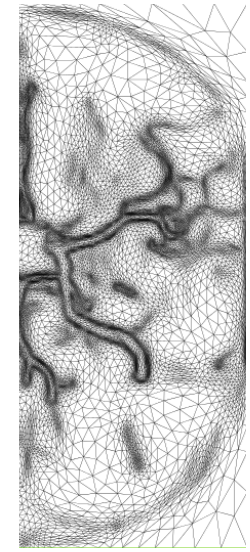

Energy functional minimization combined with an anisotropic mesh adaptation

Simona Perotto

MOX-Modeling and Scientific Computing
Department of Mathematics, Politecnico di Milano

February 5, 2019

SAPIENZA
UNIVERSITÀ DI ROMA

crack propagation in brittle materials

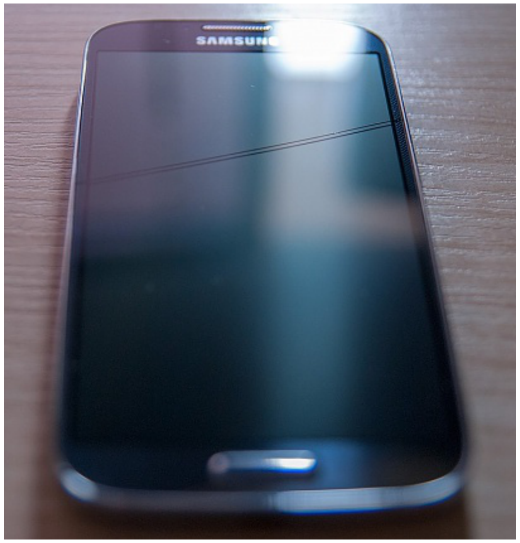
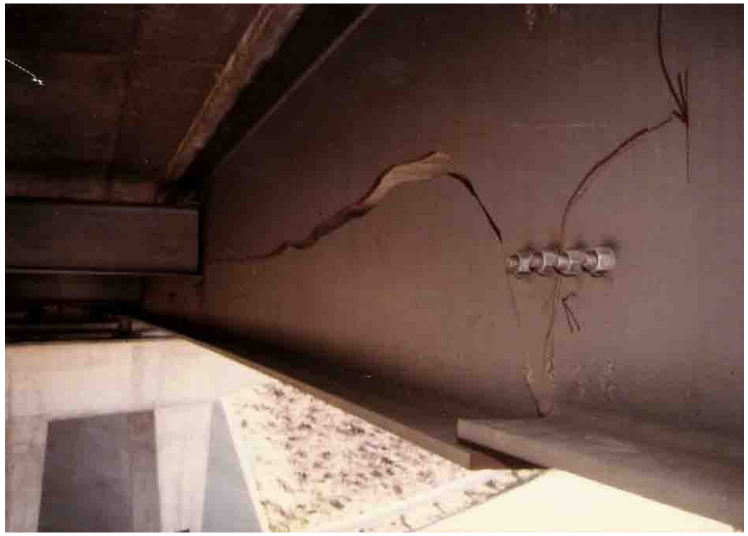
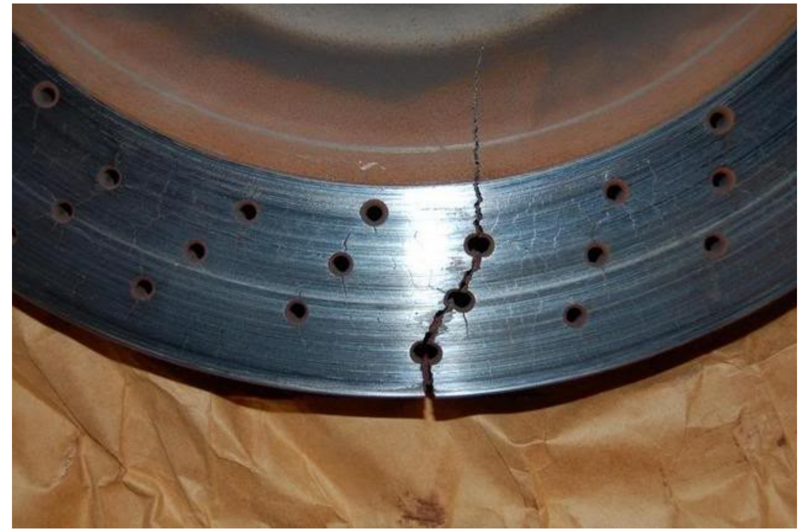

cracks $\cap$ images =energy functional minimization

image segmentation





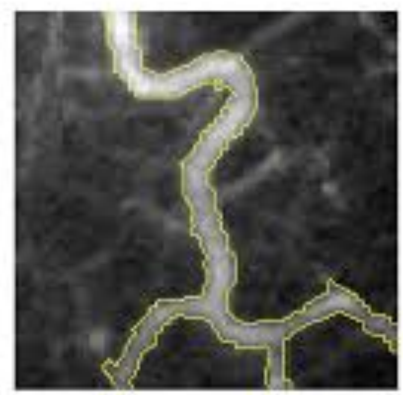

Crack propagation in brittle materials

Ambrosio-Tortorelli approximation to Francfort-Marigo model:

$$I_\varepsilon : H^1(\Omega) \times H^1(\Omega;[0,1]) \to \mathbb{R}$$

$$I_\varepsilon(u,v) = \underbrace{\int_\Omega (v^2+\eta)|\nabla u|^2\,d\mathbf{x}}_{\text{elastic energy}} + \kappa \underbrace{\int_\Omega \left[\frac{1}{4\varepsilon}(1-v)^2 + \varepsilon|\nabla v|^2\right] d\mathbf{x}}_{\text{fictitious crack energy}}$$

- $0 < \eta \ll \varepsilon \ll 1$
- $\kappa > 0$
- $v \in H^1(\Omega;[0,1])$ (phase field)
- $u \in \mathcal{A}(g(t))$ (body displacement)

1 : sound material

0 : crack

$$\mathcal{A}(g(t)) = \{u \in H^1(\Omega) : u|_{\Omega_{D\pm}} = g(t)|_{\Omega_{D\pm}}\}$$

admissible displacements

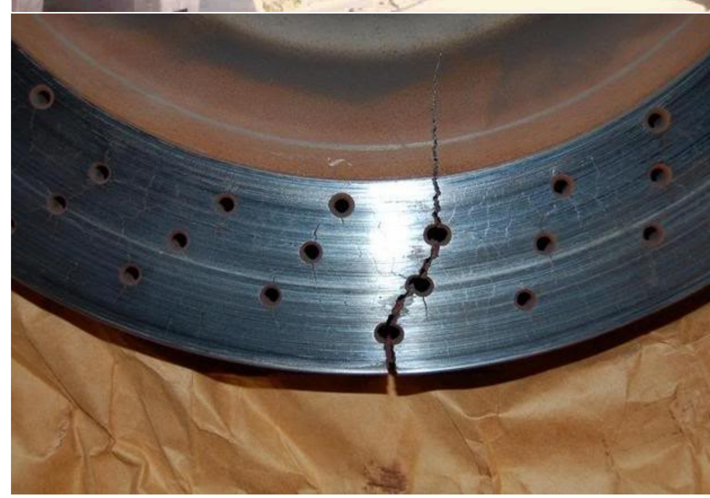

$$g : [0,T] \times \Omega \to \mathbb{R} \quad : \quad g(t) = \begin{cases} t & \text{on } \Omega_{D+}, \\ -t & \text{on } \Omega_{D-}, \\ 0 & \text{elsewhere,} \end{cases}$$

[L. Ambrosio, V.M. Tortorelli (1990,1992)]

Crack propagation in brittle materials

Ambrosio-Tortorelli approximation to Francfort-Marigo model:

$$I_\varepsilon : H^1(\Omega) \times H^1(\Omega; [0,1]) \to \mathbb{R}$$

$$I_\varepsilon(u,v) = \underbrace{\int_\Omega (v^2+\eta)|\nabla u|^2\, d\mathbf{x}}_{\text{elastic energy}} + \kappa \underbrace{\int_\Omega \left[\frac{1}{4\varepsilon}(1-v)^2 + \varepsilon|\nabla v|^2\right] d\mathbf{x}}_{\text{fictitious crack energy}}$$

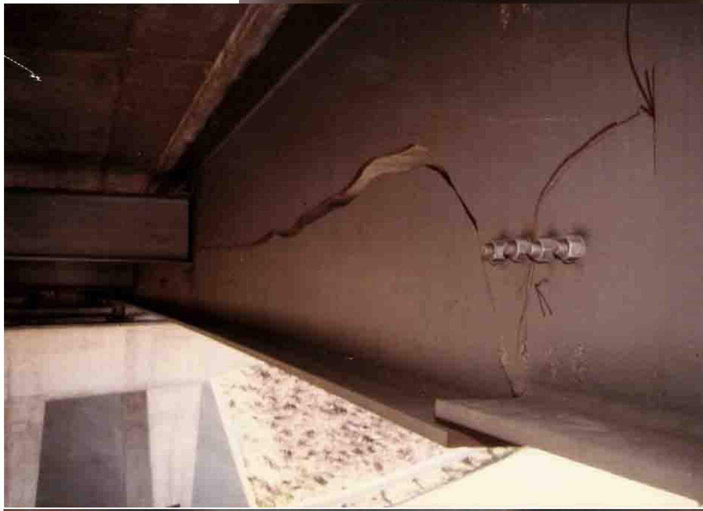

Theoretical investigation :

- Γ- convergence to Francfort-Marigo functional;
  [B. Bourdin, G.A. Francfort, J.-J. Marigo (2000)]
- existence of minimizers for $I_\varepsilon(u,v)$ ($\varepsilon, \eta > 0$);
  [L. Ambrosio, V.M. Tortorelli (1992)]

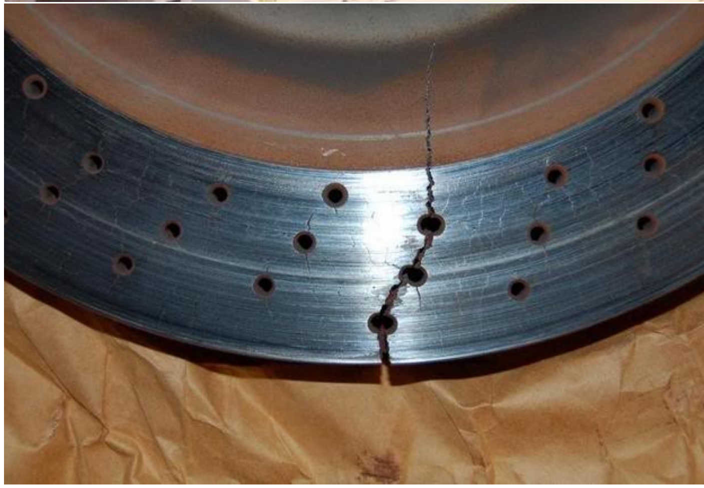

[L. Ambrosio, V.M. Tortorelli (1990,1992)]

Crack propagation in brittle materials

Ambrosio-Tortorelli approximation to Francfort-Marigo model:

$$I_\varepsilon : H^1(\Omega) \times H^1(\Omega;[0,1]) \to \mathbb{R}$$

$$I_\varepsilon(u,v) = \underbrace{\int_\Omega (v^2+\eta)|\nabla u|^2 \, d\mathbf{x}}_{\text{elastic energy}} + \kappa \underbrace{\int_\Omega \left[\frac{1}{4\varepsilon}(1-v)^2 + \varepsilon |\nabla v|^2\right] d\mathbf{x}}_{\text{fictitious crack energy}}$$

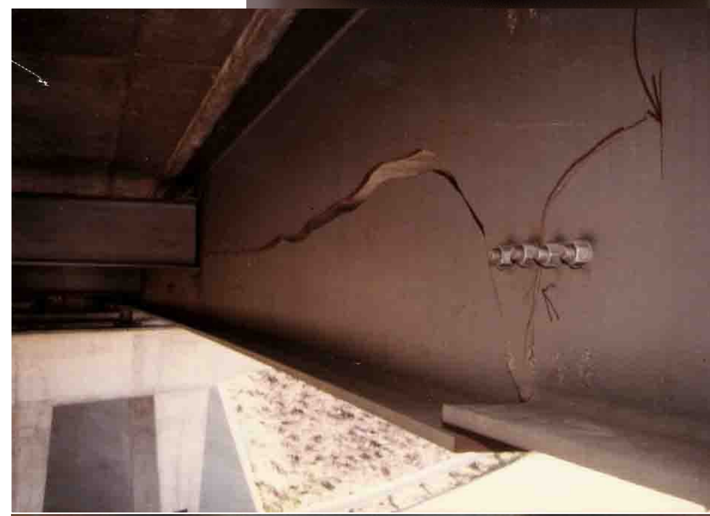

Crack evolution :

- time discretization : $0 = t_0 < t_1 < \cdots < t_F = T$
- minimization at each time step: $\boxed{t = t_0}$

$$(u_\varepsilon(t_0), v_\varepsilon(t_0)) \in \underset{\substack{u \in \mathcal{A}(g(t_0)),\\ v \in H^1(\Omega;[0,1])}}{\arg\min} I_\varepsilon(u,v)$$

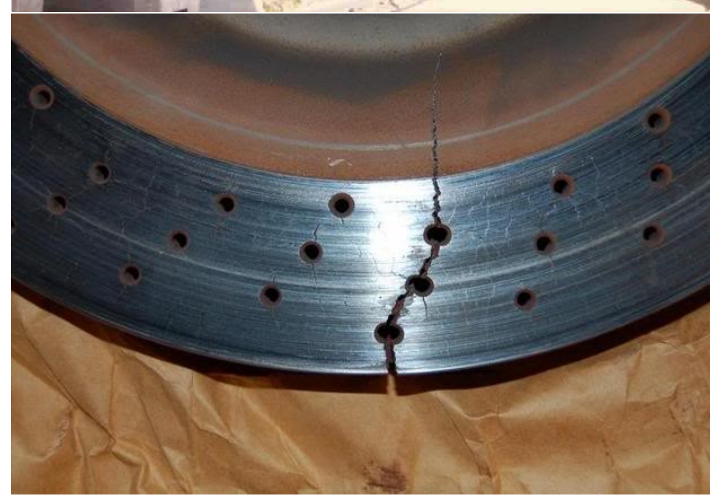

quasi-static approach

[L. Ambrosio, V.M. Tortorelli (1990,1992)]

Crack propagation in brittle materials

Ambrosio-Tortorelli approximation to Francfort-Marigo model:

$$I_\varepsilon : H^1(\Omega) \times H^1(\Omega; [0,1]) \to \mathbb{R}$$

$$I_\varepsilon(u,v) = \underbrace{\int_\Omega (v^2+\eta)|\nabla u|^2 \, d\mathbf{x}}_{\text{elastic energy}} + \kappa \underbrace{\int_\Omega \left[\frac{1}{4\varepsilon}(1-v)^2 + \varepsilon|\nabla v|^2\right] d\mathbf{x}}_{\text{fictitious crack energy}}$$

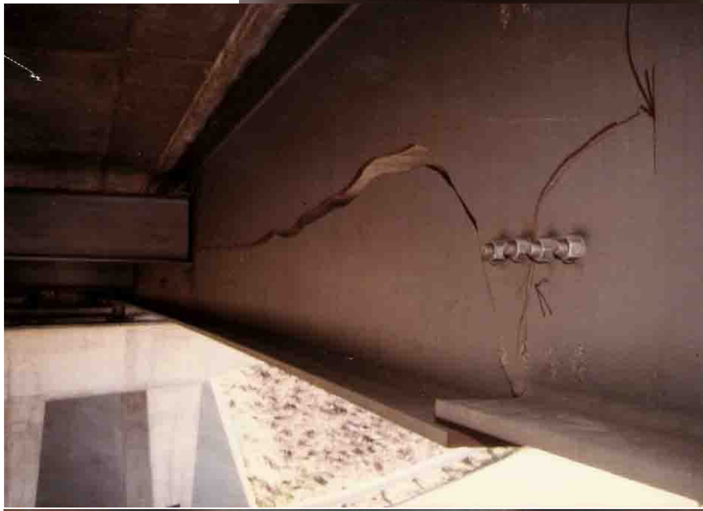

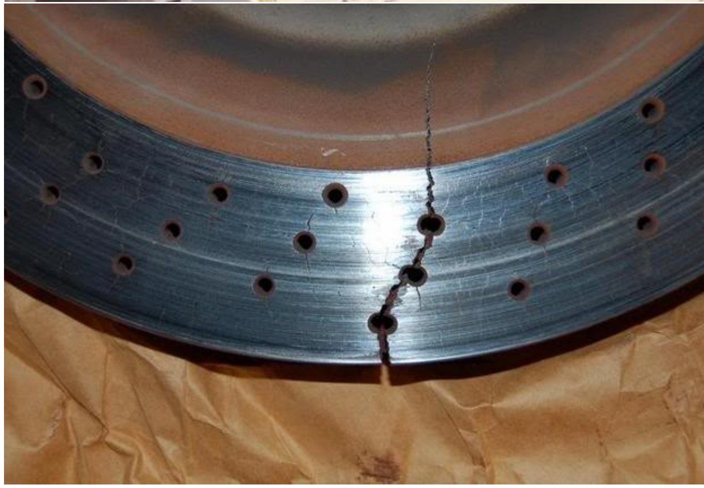

Crack evolution :

- **time discretization :** $0 = t_0 < t_1 < \cdots < t_F = T$
- **minimization at each time step:** $\boxed{t = t_k}$

$$(u_\varepsilon(t_k), v_\varepsilon(t_k)) \in \underset{\substack{u \in \mathcal{A}(g(t_k)),\\ v \in H^1(\Omega;[0,1]),\, v \le v_\varepsilon(t_{k-1})}}{\arg\min} I_\varepsilon(u,v)$$

irreversibility of the crack

[A. Giacomini (2005)]

quasi-static approach

[L. Ambrosio, V.M. Tortorelli (1990,1992)]

The modified Ambrosio-Tortorelli model

[M. Artina, M. Fornasier, S. Micheletti, S.P. (2015a)]

Idea : relax the constraints on the displacement and on the phase field via penalization:

$$\boxed{u, v \in H^1(\Omega)}$$

[B. Bourdin (2007)]

- $v \leq v_\varepsilon(t_{k-1})$ $\Longrightarrow$ **equality** constraint. If at $t = t_{k-1}$

$$CR_{k-1} = \{\mathbf{x} \in \bar{\Omega} \,|\, v_\varepsilon(t_{k-1}) < \mathtt{CRTOL}\} \neq \emptyset$$

the **irreversibility** is enforced by

$$\boxed{v_\varepsilon(\mathbf{x}, t_i) = 0 \qquad \forall \mathbf{x} \in CR_{k-1} \quad \text{and} \quad \forall i \,:\, k \leq i \leq F.}$$

$$\Downarrow$$

$$(u_\varepsilon(t_k), v_\varepsilon(t_k)) \in \underset{\substack{u \in H^1(\Omega), \\ v \in H^1(\Omega;[0,1])}}{\arg\min} \; I^{penalty}_{\varepsilon,k}(u, v) \qquad k = 1, \ldots, F$$

The modified Ambrosio-Tortorelli model

[M. Artina, M. Fornasier, S. Micheletti, S.P. (2015a)]

Idea : relax the constraints on the displacement and on the phase field via penalization.

$$\boxed{u, v \in H^1(\Omega)}$$

[B. Bourdin (2007)]

- $v \leq v_\varepsilon(t_{k-1})$ $\longrightarrow$ **equality** constraint. If at $t = t_{k-1}$

$$CR_{k-1} = \{\mathbf{x} \in \bar{\Omega} \,|\, v_\varepsilon(t_{k-1}) < \mathtt{CRTOL}\} \neq \emptyset,$$

the **irreversibility** is enforced by

$$\boxed{v_\varepsilon(\mathbf{x}, t_i) = 0 \qquad \forall \mathbf{x} \in CR_{k-1} \quad \text{and} \quad \forall i \,:\, k \leq i \leq F.}$$

$$\Downarrow$$

$$I^{penalty}_{\varepsilon,k}(u,v) = \int_\Omega (v^2 + \eta)|\nabla u|^2 \, d\mathbf{x} + \kappa \int_\Omega \left[\frac{1}{4\varepsilon}(1-v)^2 + \varepsilon|\nabla v|^2\right] d\mathbf{x}$$

$$+ \underbrace{\frac{1}{\gamma_A}\int_{\Omega_{D\pm}} (g(t_k) - u)^2 \, d\mathbf{x}}_{\text{admissible displacement}} + \underbrace{\frac{1}{\gamma_B}\int_{CR_{k-1}} v^2 \, d\mathbf{x},}_{\text{irreversibility}}$$

The modified Ambrosio-Tortorelli model

[M. Artina, M. Fornasier, S. Micheletti, S.P. (2015a)]

Idea : relax the constraints on the displacement and on the phase field via penalization.

$$\boxed{u, v \in H^1(\Omega)}$$

[B. Bourdin (2007)]

- $v \leq v_\varepsilon(t_{k-1})$ ⟶ **equality** constraint. If at $t = t_{k-1}$

$$CR_{k-1} = \{\mathbf{x} \in \bar{\Omega} \,|\, v_\varepsilon(t_{k-1}) < \mathtt{CRTOL}\} \neq \emptyset,$$

the **irreversibility** is enforced by

$$\boxed{v_\varepsilon(\mathbf{x}, t_i) = 0 \qquad \forall \mathbf{x} \in CR_{k-1} \quad \text{and} \quad \forall i \, : \, k \leq i \leq F.}$$

⬇

$$(u_\varepsilon(t_k), v_\varepsilon(t_k)) \in \underset{\substack{u \in H^1(\Omega), \\ v \in H^1(\Omega;[0,1])}}{\arg\min} \quad I^{penalty}_{\varepsilon,k}(u, v) \qquad k = 1, \ldots, F$$

$$\boxed{v \in H^1(\Omega;[0,1])}$$

automatically fulfilled

The modified Ambrosio-Tortorelli model

[M. Artina, M. Fornasier, S. Micheletti, S.P. (2015a)]

$$\begin{aligned} I(u,v) &= \int_\Omega \left[(v^2+\eta)|\nabla u|^2\,d\mathbf{x} + \alpha(1-v)^2 + \varepsilon|\nabla v|^2\right]\,d\mathbf{x} \\ &+ \frac{1}{\gamma_A}\int_{\Omega_{D\pm}} (g(t_k)-u)^2\,d\mathbf{x} + \frac{1}{\gamma_B}\int_{CR_{k-1}} v^2\,d\mathbf{x} \end{aligned}$$

[S. Burke, Ch. Ortner, E. Süli (2010)]

Looking for critical points : Fréchet differentiable

$$\begin{aligned} I'(w,z;\varphi,\psi) = \;& 2\left(\int_\Omega (z^2+\eta)\nabla w\cdot\nabla\varphi\,d\mathbf{x} + \frac{1}{\gamma_A}\int_{\Omega_{D\pm}} (w-g(t_k))\varphi\,d\mathbf{x}\right) \\ & + 2\left(\int_\Omega \left[z\psi|\nabla w|^2 + \alpha(z-1)\psi + \varepsilon\nabla z\cdot\nabla\psi\right]d\mathbf{x} + \frac{1}{\gamma_B}\int_{CR_{k-1}} z\psi\,d\mathbf{x}\right) \\ =: \;& 2a_{\gamma_A}(z;w,\varphi) + 2b_{\gamma_B}(w;z,\psi) \end{aligned}$$

If $(u,v)\in H^1(\Omega)\times(H^1(\Omega)\cap L^\infty(\Omega))$ **is a critical point, then** $0\le v(\mathbf{x})\le 1$ **a.e. in** Ω.

discrete counterpart

The discrete modified Ambrosio-Tortorelli model

[M. Artina, M. Fornasier, S. Micheletti, S.P. (2015a)]

$$
\begin{aligned}
I_h(u_h, v_h) \quad &= \quad \int_\Omega \Big[\big(P_h(v_h^2) + \eta\big) \, |\nabla u_h|^2 \, d\mathbf{x} + \alpha P_h((1 - v_h)^2) + \varepsilon |\nabla v_h|^2 \Big] \, d\mathbf{x} \\
&+ \quad \frac{1}{\gamma_A} \int_{\Omega_{D\pm}} P_h\left((g_h(t_k) - u_h)^2\right) \, d\mathbf{x} + \frac{1}{\gamma_B} \int_{CR_{k-1}} P_h\left(v_h^2\right) \, d\mathbf{x}.
\end{aligned}
$$

$P_h \, : \, C^0(\overline{\Omega}) \to X_h$ **(Lagrangian interpolant)** **+ hypotheses on g_h and on the stiffness matrix**

Looking for critical points : Fréchet differentiable

$$
\begin{aligned}
I'_h(u_h, v_h; \varphi_h, \psi_h) = 2\bigg(&\int_\Omega (P_h(v_h^2) + \eta) \nabla u_h \cdot \nabla \varphi_h \, d\mathbf{x} + \frac{1}{\gamma_A} \int_{\Omega_{D\pm}} P_h((u_h - g_h(t_k))\varphi_h) \, d\mathbf{x} \bigg) \\
&+ 2\bigg(\int_\Omega \Big[P_h(v_h \psi_h) |\nabla u_h|^2 + \alpha P_h((v_h - 1)\psi_h) + \varepsilon \nabla v_h \cdot \nabla \psi_h \Big] \, d\mathbf{x} \\
&+ \frac{1}{\gamma_B} \int_{CR^h_{k-1}} P_h\left(v_h \psi_h\right) \, d\mathbf{x} \bigg) =: 2a^h_{\gamma_A}(v_h; u_h, \varphi_h) + 2b^h_{\gamma_B}(u_h; v_h, \psi_h)
\end{aligned}
$$

If $(u_h, v_h) \in X_h \times X_h$, with X_h the P1-finite element space, is a critical point, then $0 \le v_h \le 1$ in Ω.

MOX

How to select the mesh?

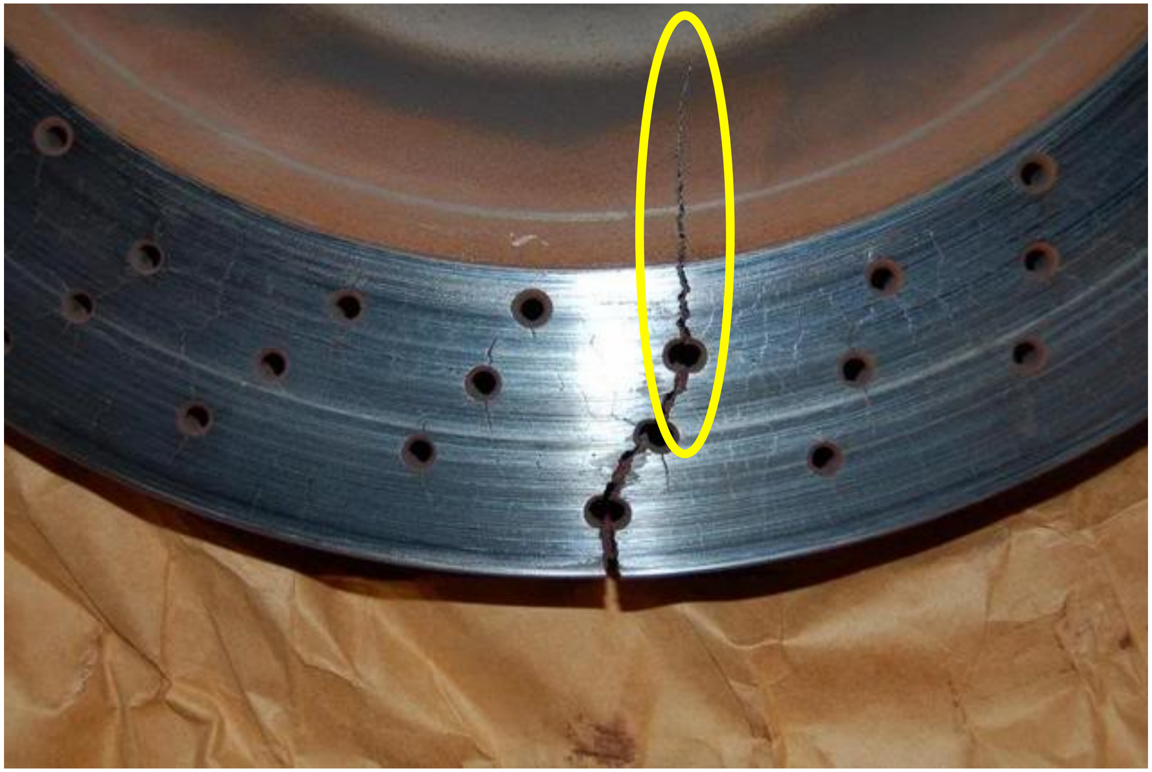

sharp features to be captured

anisotropic adapted meshes
sharply capture these features

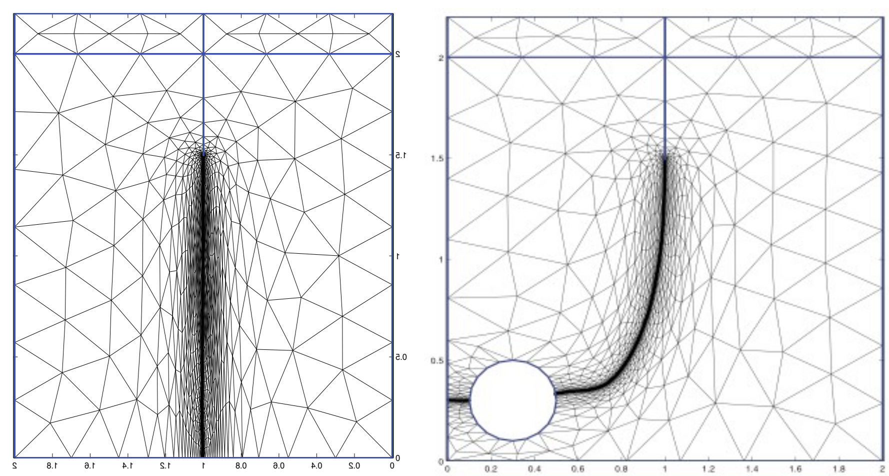

reduce the dofs (or increase the accuracy) by tuning size, shape and orientation of mesh elements

[e.g., M. Fortin, J. Dompierre, W.G. Habashi, M.G. Vallet et al. (2000,2002)]

Anisotropic mesh adaptation

looking for anisotropic information

[L. Formaggia, S.P. (2001)]

interpolation error estimates

[L. Formaggia, S.P. (2001,2003)]

error indicators/estimators

[L. Formaggia, S.P. (2003); S. Micheletti, S.P. (2008,2010,2011); P.E. Farrell, S. Micheletti, S.P.(2010); M. Artina, M. Fornasier, S. Micheletti, S.P. (2015)]

adaptation procedure

*[L. Formaggia, S.P. (2001);
L. Formaggia, S. Micheletti, S.P. (2004)]*

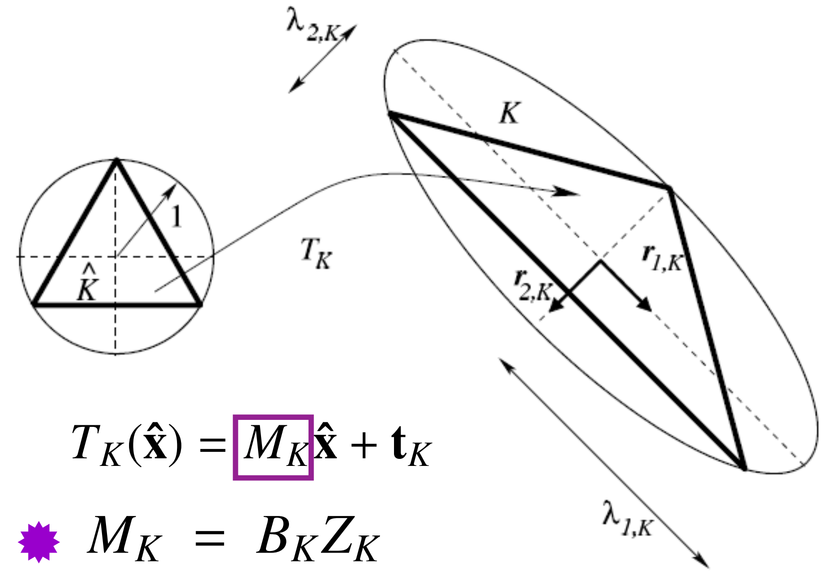

$$T_K(\hat{\mathbf{x}}) = \boxed{M_K}\hat{\mathbf{x}} + \mathbf{t}_K$$

- $M_K = B_K Z_K$
- $B_K = R_K^T \Lambda_K R_K,$

$$R_K^T = [\mathbf{r}_{1,K}, \mathbf{r}_{2,K}]$$
$$\Lambda_K = \mathrm{diag}(\lambda_{1,K}, \lambda_{2,K})$$

$$\boxed{s_K = \lambda_{1,K}/\lambda_{2,K}}$$

Anisotropic mesh adaptation

looking for anisotropic information

[L. Formaggia, S.P. (2001)]

interpolation error estimates

[L. Formaggia, S.P. (2001,2003)]

error indicators/estimators

[L. Formaggia, S.P. (2003); S. Micheletti, S.P. (2008,2010,2011); P.E. Farrell, S. Micheletti, S.P.(2010); M. Artina, M. Fornasier, S. Micheletti, S.P. (2015)]

adaptation procedure

[L. Formaggia, S.P. (2001);
L. Formaggia, S. Micheletti, S.P. (2004)]

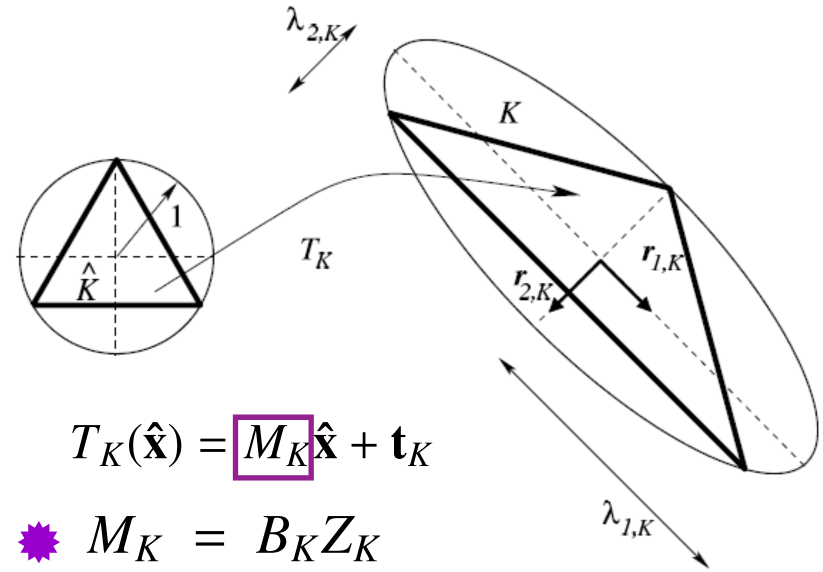

$$T_K(\hat{\mathbf{x}}) = \boxed{M_K}\hat{\mathbf{x}} + \mathbf{t}_K$$

- $M_K = B_K Z_K$
- $B_K = R_K^T \Lambda_K R_K,$

$$R_K^T = [\mathbf{r}_{1,K}, \mathbf{r}_{2,K}]$$
$$\Lambda_K = \mathrm{diag}(\lambda_{1,K}, \lambda_{2,K})$$

$$\boxed{s_K = \lambda_{1,K}/\lambda_{2,K}}$$

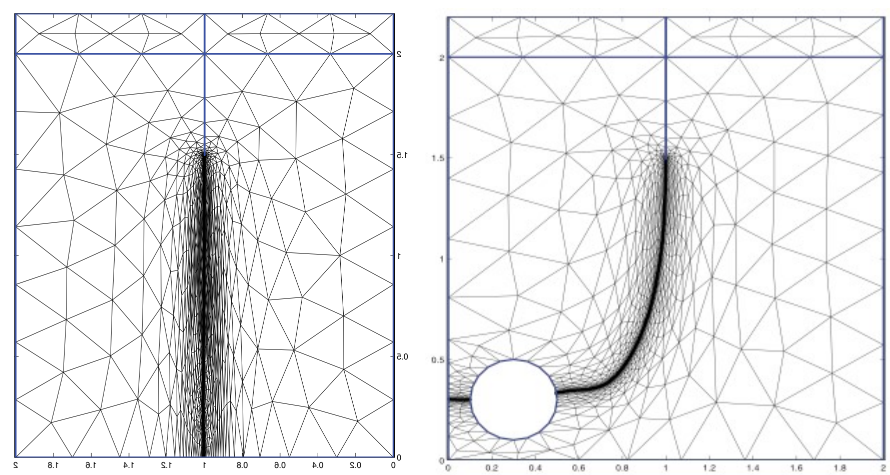

Anisotropic mesh adaptation

looking for anisotropic information

[L. Formaggia, S.P. (2001)]

interpolation error estimates

[L. Formaggia, S.P. (2001,2003)]

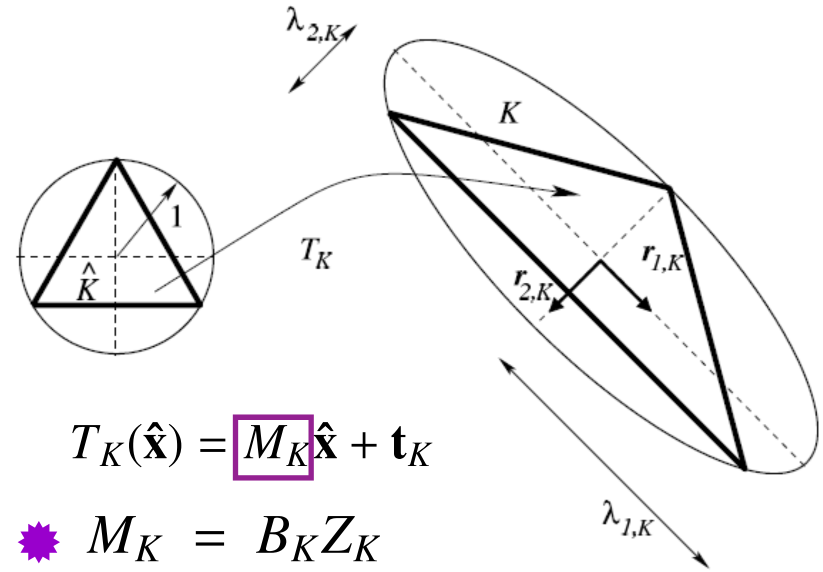

$$T_K(\hat{\mathbf{x}}) = \boxed{M_K}\hat{\mathbf{x}} + \mathbf{t}_K$$

- $M_K = B_K Z_K$
- $B_K = R_K^T \Lambda_K R_K,$

$$R_K^T = [\mathbf{r}_{1,K}, \mathbf{r}_{2,K}]$$
$$\Lambda_K = \mathrm{diag}(\lambda_{1,K}, \lambda_{2,K})$$

$$[G_K(\mathbf{w})]_{i,j} = \sum_{T \in \Delta_K} \int_T w_i w_j \, d\mathbf{x}, \quad \text{with } i,j = 1,2$$

$$\boxed{s_K = \lambda_{1,K}/\lambda_{2,K}}$$

A $$\|v - I_K^1(v)\|_{L^2(K)} \leq C_1^* \Big(\sum_{i=1}^{2} \lambda_{i,K}^2 (\mathbf{r}_{i,K}^T \boxed{G_K(\nabla v)} \mathbf{r}_{i,K}) \Big)^{1/2}$$

I $$\|v - I_K^1(v)\|_{L^2(K)} \leq C_1 h_K \boxed{|v|_{H^1(\Delta_K)}}$$

An anisotropic a posteriori error estimator

[M. Artina, M. Fornasier, S. Micheletti, S.P. (2015a)]

Goal : set an optimization procedure to minimize $I(u,v)$ by successive minimizations of $I_h(u_h, v_h)$ on anisotropic meshes.

$$\boxed{|I'(u_h, v_h; \varphi, \psi)|}$$

[S. Burke, Ch.. Ortner, E. Süli. (2010)]

$$\underbrace{|I'(u_h, v_h; \varphi, \psi)|}_{\text{critical point of } I_h} \le C \sum_{K\in\mathcal{T}_h} \{\underbrace{\rho_K^A(v_h,u_h)}_{\text{residual}}\,\omega_K(\varphi) + \underbrace{\rho_K^B(u_h,v_h)}_{\text{residual}}\,\omega_K(\psi)\}$$

$$\forall \varphi, \psi \in H^1(\Omega)$$

$$\begin{aligned}
\rho_K^A(v_h,u_h) = {} & \frac{1}{2}\|[\![\nabla u_h]\!]\|_{L^\infty(\partial K)}\,\|v_h^2+\eta\|_{L^2(\partial K)}\left(\frac{h_K}{\lambda_{1,K}\lambda_{2,K}}\right)^{\frac{1}{2}} \\
& + \|2v_h(\nabla v_h\cdot\nabla u_h)\|_{L^2(K)} + \frac{\delta_{K,\Omega_D^\pm}}{\gamma_A}\Big(\|u_h - g_h(t_k)\|_{L^2(K)} \\
& + \|g_h(t_k) - g(t_k)\|_{L^2(K)}\Big) + \frac{1}{\lambda_{2,K}}\Big[\|v_h^2 - P_h(v_h^2)\|_{L^\infty(K)}\,\|\nabla u_h\|_{L^2(K)} \\
& + \frac{|K|^{1/2}\,h_K^2}{\gamma_A}\,|u_h - g_h(t_k)|_{W^{1,\infty}(K)}\Big]
\end{aligned}$$

$$\begin{aligned}
\rho_K^B(u_h,v_h) = {} & \|(|\nabla u_h|^2+\alpha)v_h - \alpha\|_{L^2(K)} + \frac{\varepsilon}{2}\,\|[\![\nabla v_h]\!]\|_{L^2(\partial K)}\left(\frac{h_K}{\lambda_{1,K}\lambda_{2,K}}\right)^{1/2} \\
& + \frac{\delta_{K,CR_{k-1}}}{\gamma_B}\,\|v_h\|_{L^2(K)} + \frac{h_K^2}{\lambda_{2,K}}\Big[\|\,|\nabla u_h|^2+\alpha\|_{L^2(K)} \\
& + \frac{|K|^{1/2}\,\delta_{K,CR_{k-1}}}{\gamma_B}\Big]\,|v_h|_{W^{1,\infty}(K)}
\end{aligned}$$

An anisotropic a posteriori error estimator

[M. Artina, M. Fornasier, S. Micheletti, S.P. (2015a)]

Goal : set an optimization procedure to minimize $I(u,v)$ by successive minimizations of $I_h(u_h, v_h)$ on anisotropic meshes.

$$\boxed{|I'(u_h, v_h; \varphi, \psi)|}$$

[S. Burke, Ch.. Ortner, E. Süli. (2010)]

$$|I'(\underbrace{u_h, v_h}_{\text{critical point of } I_h}; \varphi, \psi)| \le C \sum_{K\in\mathcal{T}_h} \{\rho_K^A(v_h, u_h)\underbrace{\omega_K(\varphi)}_{\text{weight}} + \rho_K^B(u_h, v_h)\underbrace{\omega_K(\psi)}_{\text{weight}}\}$$

$$\forall \varphi, \psi \in H^1(\Omega)$$

$$\boxed{\omega_K(w) = \Big[\sum_{i=1}^{2} \lambda_{i,K}^2 (\mathbf{r}_{i,K}^T G_{\Delta_K}(w)\mathbf{r}_{i,K})\Big]^{1/2}}$$

$$\left.\begin{aligned} \varphi &= u - u_h \\ \psi &= v - v_h \end{aligned}\right\} \quad I(u,v) - I(u_h, v_h) = \frac{1}{2} I'(u_h, v_h; u - u_h, v - v_h) + \underbrace{R}_{\substack{\text{third order} \\ \text{remainder}}}$$

+ gradient recovery procedures

[O.C. Zienkiewicz, J.Z. Zhu (1987,1992)]

MOX

The numerical procedure

[M. Artina, M. Fornasier, S. Micheletti, S.P. (2015a)]

$$
\begin{aligned}
I(u,v) &= \int_\Omega \left[(\boxed{v^2} + \eta) \boxed{|\nabla u|^2}\, d\mathbf{x} + \alpha (1-v)^2 + \varepsilon |\nabla v|^2 \right]\, d\mathbf{x} \\
&+ \frac{1}{\gamma_A} \int_{\Omega_{D\pm}} (g(t_k) - u)^2 \, d\mathbf{x} + \frac{1}{\gamma_B} \int_{CR_{k-1}} v^2 \, d\mathbf{x}
\end{aligned}
$$

non-convex functional

The (alternate) minimization algorithm :

1. *Set* $k = 0$;
2. *If* $k = 0$, *set* $v^1 = 1$; *else* $v^1 = v(t_{k-1})$.
3. *Set* $i = 1$; $err = 1$;

while $err \geq \texttt{VTOL}$ ***do***

    4. $u^i = \underset{z \in H^1(\Omega)}{\arg\min}\, I(z, v^i)$;

    5. $v^{i+1} = \underset{z \in H^1(\Omega)}{\arg\min}\, I(u^i, z)$;

    6. $err = \|v^{i+1} - v^i\|_{L^\infty(\Omega)}$;

    7. $i \leftarrow i + 1$;

end while

8. $u(t_k) = u^{i-1}$; $v(t_k) = v^i$;
9. $k \leftarrow k + 1$;
10. *if* $k > F$, *stop*; *else goto* 2.

two separate convex minimizations

[B. Bourdin (2007), B. Bourdin, G.A. Francfort, J.-J. Marigo (2000), S. Burke, Ch. Ortner, E. Süli (2010)]

How to make effective an error estimator: a metric-based approach

[L. Formaggia, S.P. (2001); L. Formaggia, S. Micheletti, S. P. (2004)]

CRITERION : minimize the number of the mesh elements for a fixed accuracy

+ error equidistribution

estimator $\longrightarrow$ *metric* $\longrightarrow$ *adapted mesh*

predictive procedure:
"Mesh is not a data but an unknown of the problem" (M. Fortin)

At each step of the adaptive process:

- the actual mesh $\mathcal{T}_h^{(j)}$; *approximation of the differential problem*
- the predicted (piecewise constant) metric $\widetilde{M}^{(j+1)}$ computed on $\mathcal{T}_h^{(j)}$;
- the updated mesh $\mathcal{T}_h^{(j+1)}$.

MOX

How to make effective an error estimator: a metric-based approach

[L. Formaggia, S.P. (2001); L. Formaggia, S. Micheletti, S. P. (2004)]

CRITERION : minimize the number of the mesh elements for a fixed accuracy

+ error equidistribution

estimator $\Longrightarrow$ *metric* $\Longrightarrow$ *adapted mesh*

predictive procedure:
"Mesh is not a data but an unknown of the problem" (M. Fortin)

At each step of the adaptive process:

local optimization problems

- the actual mesh $\mathcal{T}_h^{(j)}$;

construction of the error estimator

- the predicted (piecewise constant) metric $\widetilde{M}^{(j+1)}$ computed on $\mathcal{T}_h^{(j)}$;
- the updated mesh $\mathcal{T}_h^{(j+1)}$.

BAMG

+ stopping criterion

Merging minimization with anisotropic mesh adaptation

[M. Artina, M. Fornasier, S. Micheletti, S.P. (2015a)]

1. *Set* $k = 0$, $\mathcal{T}_h^{(1)} = \mathcal{T}_h$;
2. *If* $k = 0$, *set* $v_h^1 = 1$; *else* $v_h^1 = v_h(t_{k-1})$;
3. *Set* $i = 1$; *errmesh* $= 1$; *err* $= 1$;

while *errmesh* $>$ MESHTOL *&* *err* $>$ VTOL ***do***

4. $u_h^i = \arg\min_{z_h \in X_h^{(i)}} I(z_h, v_h^i)$;
5. $v_h^{i+1} = \arg\min_{z_h \in X_h^{(i)}} I(u_h^i, z_h)$;

minimization

6. *Compute the new metric* $\mathcal{M}^{(i+1)}$ *based on* u_h^i *and* v_h^{i+1} *with* TOL $=$ REFTOL;
7. *Build the adapted mesh* $\mathcal{T}_h^{(i+1)}$;
8. *err* $= \|v_h^{i+1} - v_h^i\|_{L^\infty(\Omega)}$;
9. *errmesh* $= |\#\mathcal{T}_h^{(i+1)} - \#\mathcal{T}_h^{(i)}| / \#\mathcal{T}_h^{(i)}$;
10. *Set* $v_h^1 = \Pi_{i \to i+1}(v_h^{i+1})$;
11. $i \leftarrow i + 1$;

end while

mesh adaptation

12. $u_h(t_k) = \Pi_{i-1 \to i}(u_h^{i-1})$; $v_h(t_k) = v_h^1$; $\mathcal{T}_h^k = \mathcal{T}_h^{(i)}$;
13. *Set* $\mathcal{T}_h^{(1)} = \mathcal{T}_h^k$;
14. $k \leftarrow k + 1$;
15. *if* $k > F$, *stop; else goto* 2.

MESHTOL : mesh stagnation VTOL : minimization check

REFTOL : accuracy on the functional

Numerical assessment: straight crack

[S. Burke, Ch. Ortner, E. Süli (2010)]

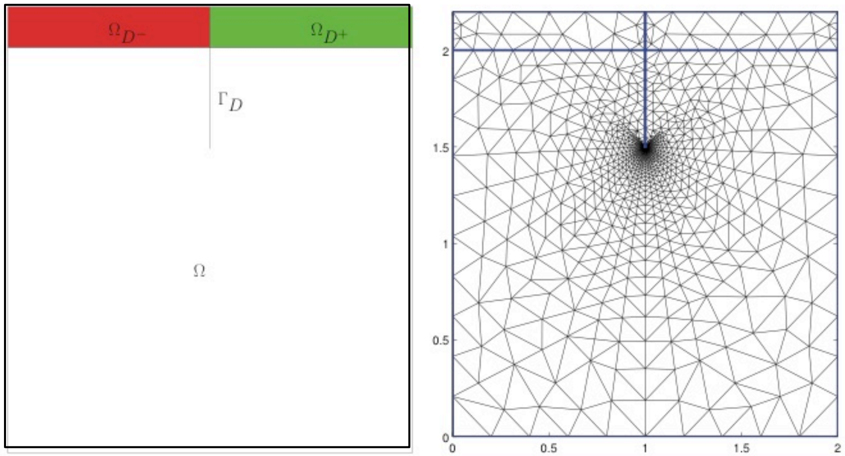

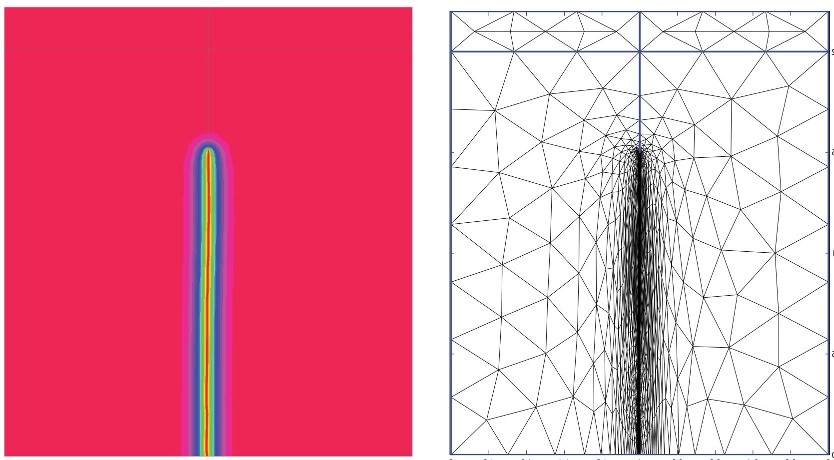

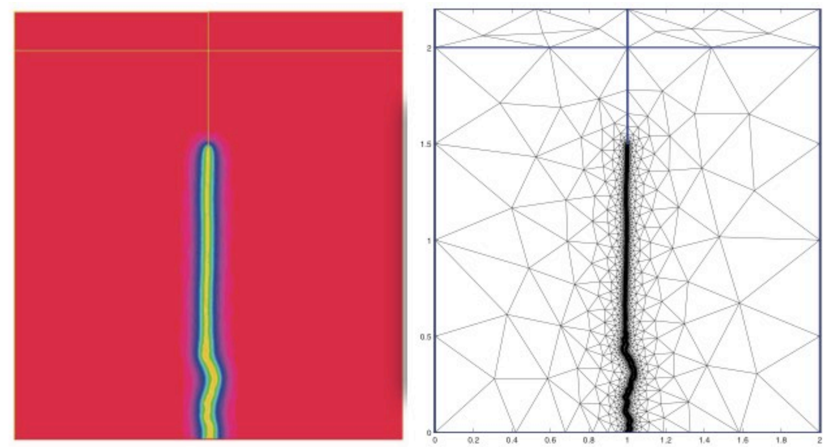

33927 elements
max aspect ratio : 1891.5

78025 elements

$\varepsilon = 2 \cdot 10^{-2}$	$\eta = 10^{-5}$	$\gamma_A = \gamma_B = 10^{-5}$	$\Delta t = 10^{-2}$
CRTOL$= 3 \cdot 10^{-4}$	VTOL$= 2 \cdot 10^{-3}$	MESHTOL$= 10^{-2}$	REFTOL$= 10^{-2}$

[M. Artina, M. Fornasier, S. Micheletti, S.P. (2015a)]

Numerical assessment: stra

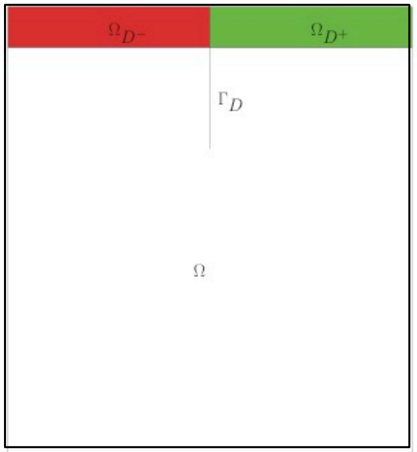

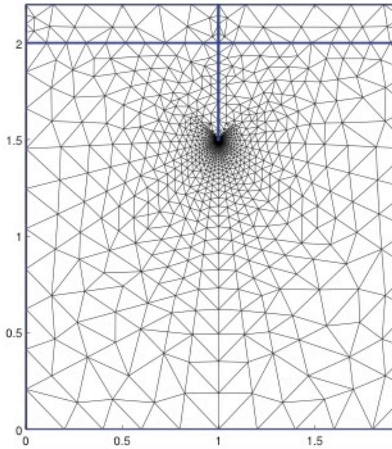

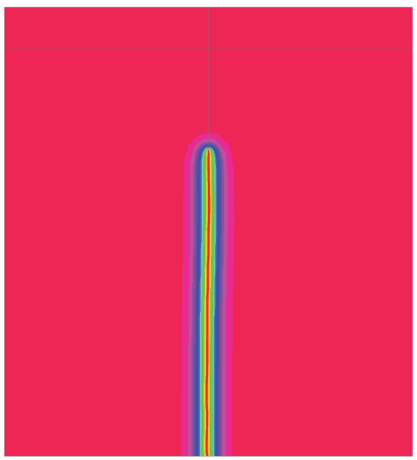

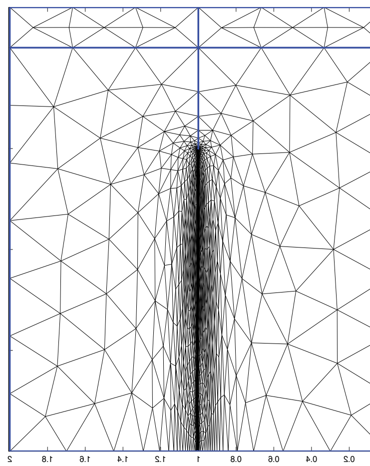

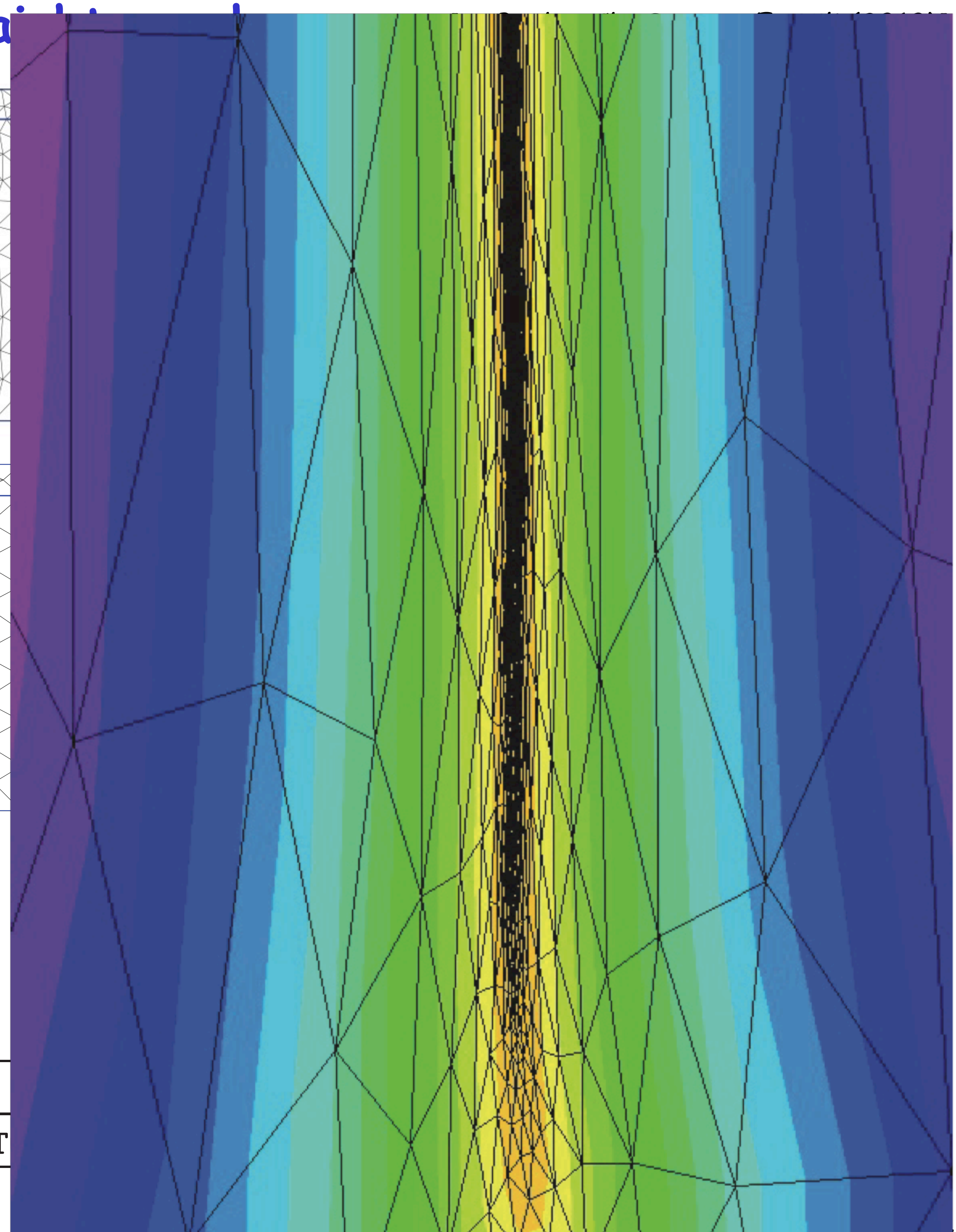

33927 elements
max aspect ratio : 1891.5

$\varepsilon = 2 \cdot 10^{-2}$	
CRTOL$= 3 \cdot 10^{-4}$	VT

[M. Artina, M. Fornasier, S. Micheletti, S.P. (2015a)]

Numerical assessment: curved crack

[S. Burke, Ch. Ortner, E. Süli (2010)]

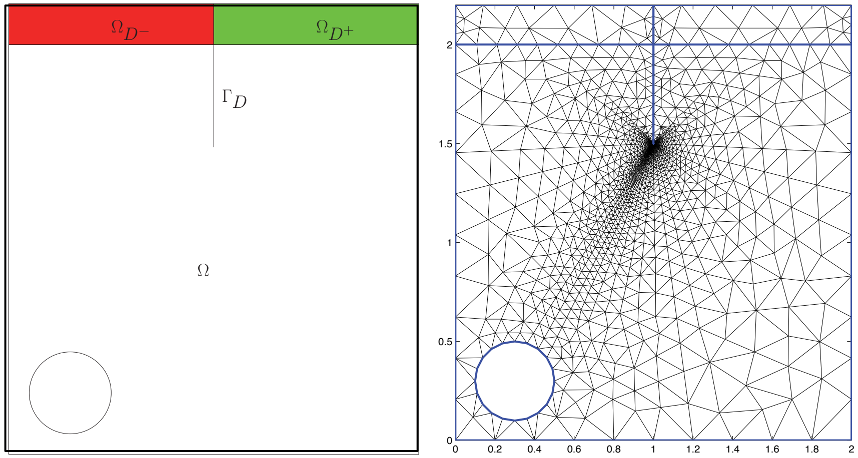

Minimization	Adaptation	Total	
192	344	536	aniso
452	765	1217	iso

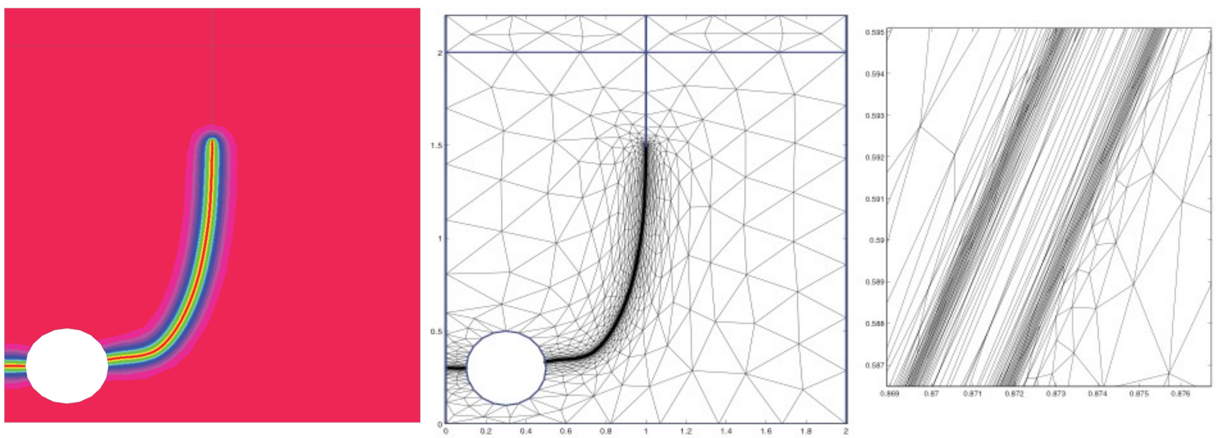

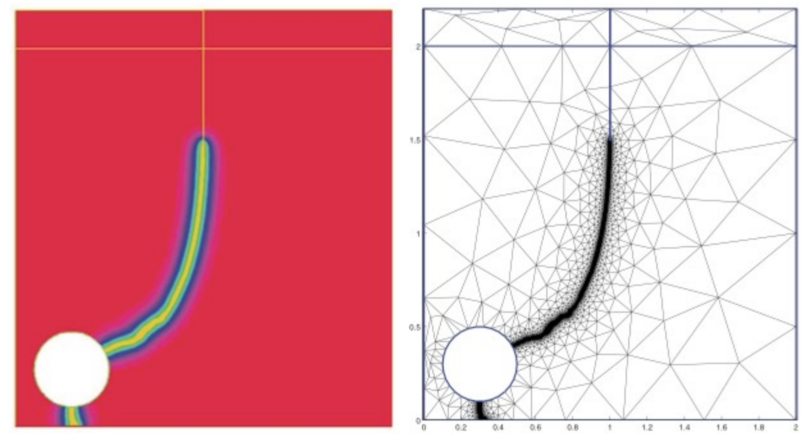

15987 elements

max aspect ratio : 1469.9

131367 elements

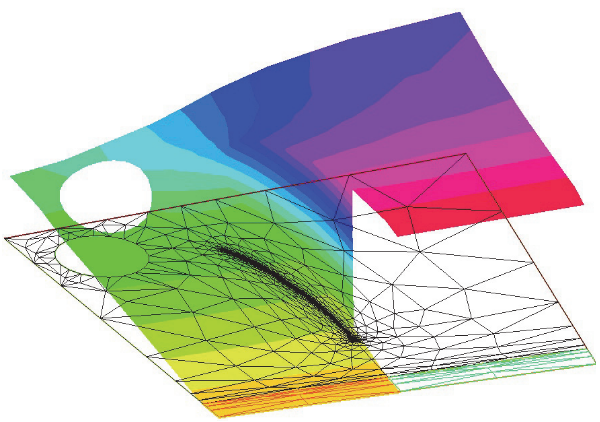

$\varepsilon = 2 \cdot 10^{-2}$	$\eta = 10^{-5}$	$\gamma_A = \gamma_B = 10^{-5}$	$\Delta t = 10^{-2}$
$\mathtt{CRTOL} = 3 \cdot 10^{-4}$	$\mathtt{VTOL} = 2 \cdot 10^{-3}$	$\mathtt{MESHTOL} = 10^{-2}$	$\mathtt{REFTOL} = 10^{-2}$

[M. Artina, M. Fornasier, S. Micheletti, S.P. (2015a)]

Variants of the basic crack model

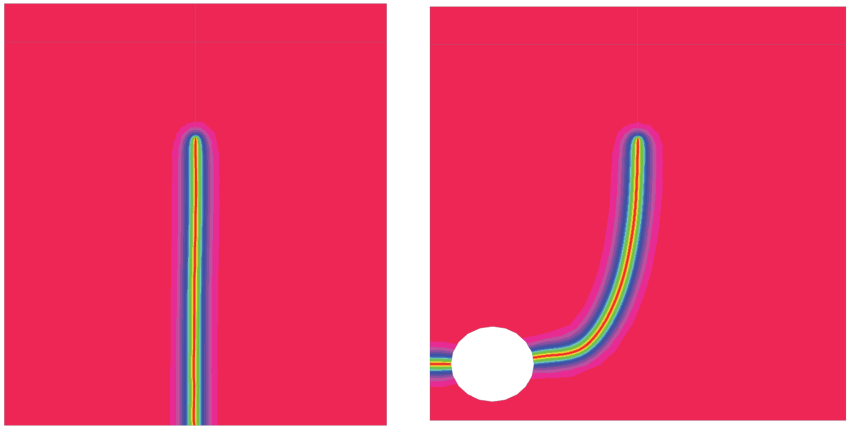

anti-plane case:
the force applied is
orthogonal to the domain

- ***Brittle fractures induced by a thermal shock.***
  [J.-J. Marigo, C. Maurini, P. Sicsic (2013), B. Bourdin, J.-J. Marigo, C. Maurini, P. Sicsic (2014)]

thermal shock is
responsible for initiation
and propagation
(the material is unnotched)

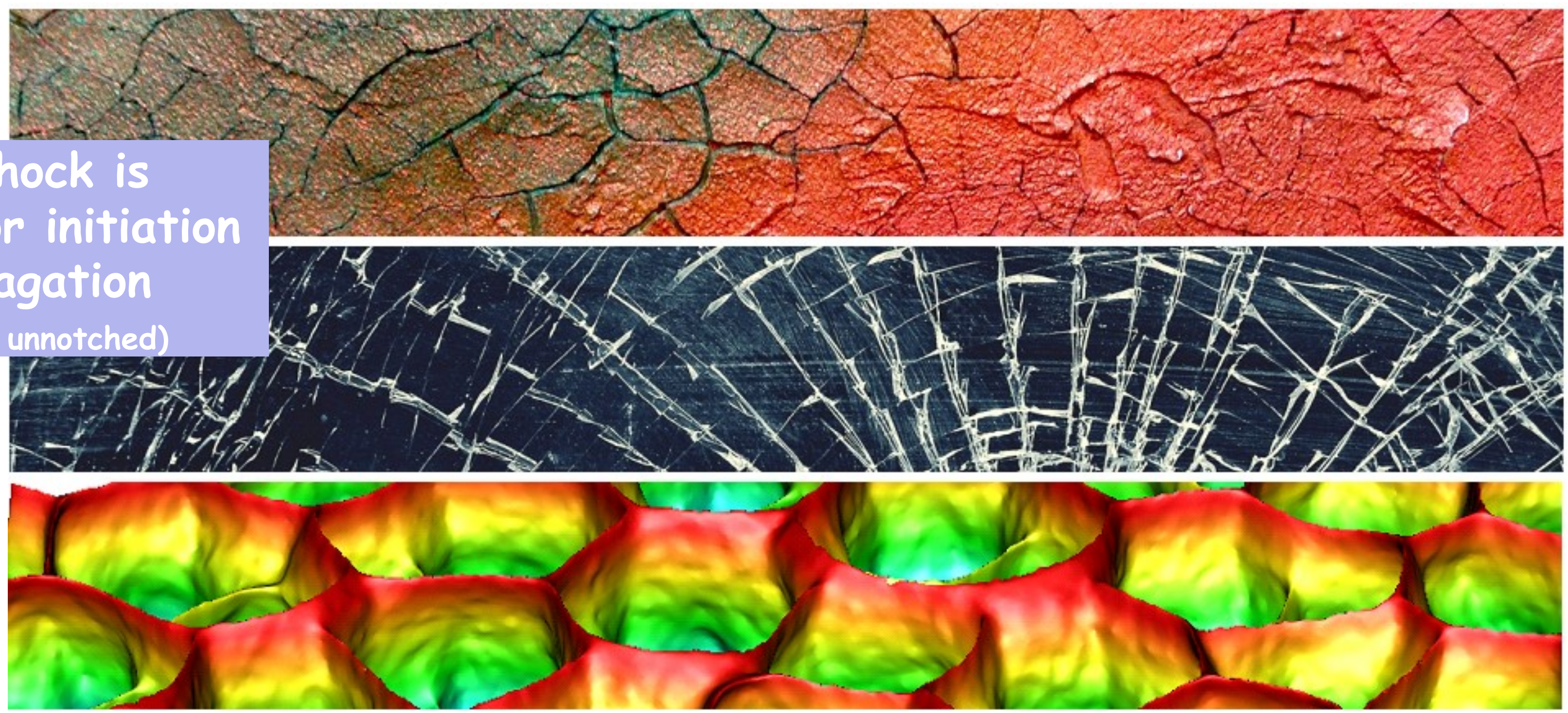

Variants of the basic crack model

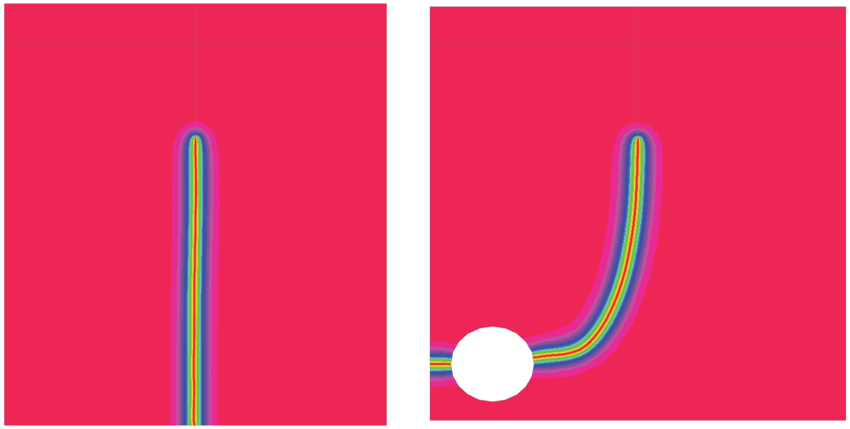

anti-plane case:
the force applied is
orthogonal to the domain

- ***Brittle fractures induced by a thermal shock.***
  [J.-J. Marigo, C. Maurini, P. Sicsic (2013), B. Bourdin, J.-J. Marigo, C. Maurini, P. Sicsic (2014)]

temperature field

$$\begin{cases} \dfrac{\partial T}{\partial t} - \nabla \cdot (k_c \nabla T) = 0 & \text{in } \Omega \times (0, t_F] \\ T = T_0 - \Delta T & \text{on } \gamma_{\text{shock}} \times (0, t_F] \\ T(\mathbf{x}, 0) = T_0 & \text{on } \Omega, \end{cases}$$

thermal diffusivity

temperature drop

thermo-mechanical model

$$\mathcal{J}(\mathbf{u}, \alpha) = \frac{1}{2} \int_\Omega (1-\alpha)^2 A(\varepsilon(\mathbf{u}) - \varepsilon_{th}) : (\varepsilon(\mathbf{u}) - \varepsilon_{th})\, d\mathbf{x} + \int_\Omega \frac{G_c}{4c_w} \left(\frac{\alpha}{l} + l\, |\nabla \alpha|^2 \right) d\mathbf{x}$$

- $\varepsilon(\mathbf{u}) = 1/2(\nabla \mathbf{u} + (\nabla \mathbf{u})^T)$ (total strain tensor)
- $\varepsilon_{th}(T) = \mu(T_0 - T)\mathbf{I}$ (inelastic strain)
- μ (thermal volumetric expansion coefficient)
- G_c (body toughness)
- A (stiffness tensor)
- l (internal length)

Variants of the basic crack model

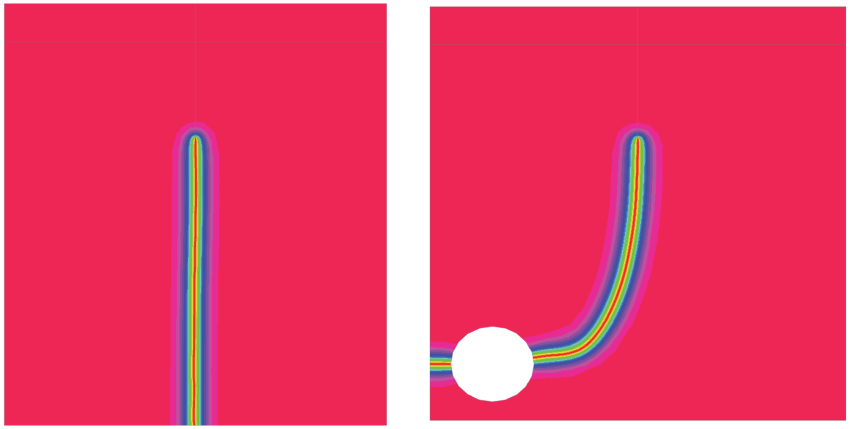

anti-plane case:
the force applied is
orthogonal to the domain

- ***Brittle fractures induced by a thermal shock effect.***

  [J.-J. Marigo, C. Maurini, P. Sicsic (2013), B. Bourdin, J.-J. Marigo, C. Maurini, P. Sicsic (2014)]

Homogeneous uniformly heated specimen, free at the boundary, no pre-stress

Three phases :

- the very early stage : a uniform strip propagates orthogonally to the immersed surface;
- at some critical time : a bifurcation occurs and the damage exhibits periodically distributed bands of equal length and grows at the center of these bands;
- later: a selective crack arrest takes place, some bands stop the others keep on propagating.

Variants of the basic crack model

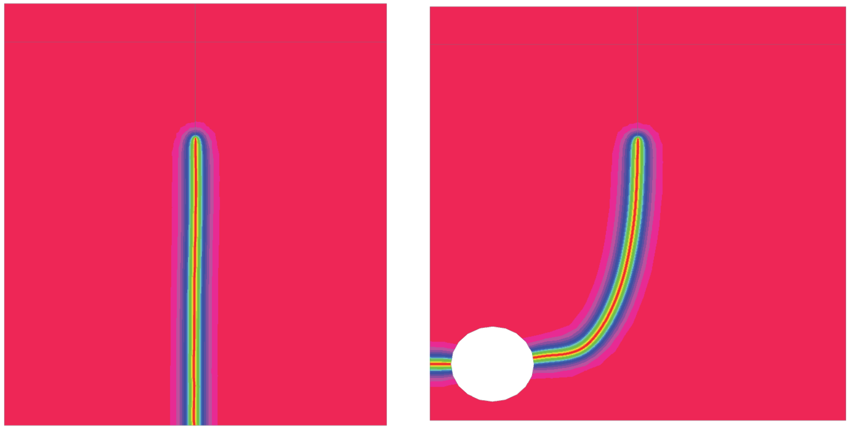

anti-plane case:
the force applied is
orthogonal to the domain

- ***Brittle fractures induced by a thermal shock effect.***

[J.-J. Marigo, C. Maurini, P. Sicsic (2013), B. Bourdin, J.-J. Marigo, C. Maurini, P. Sicsic (2014)]

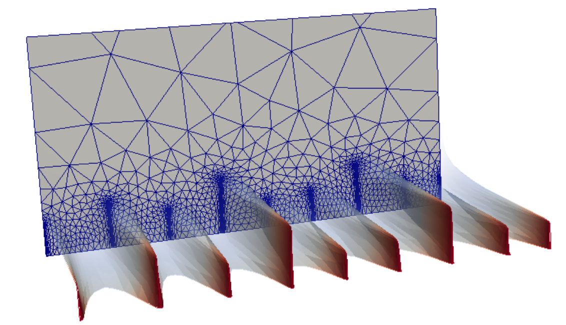

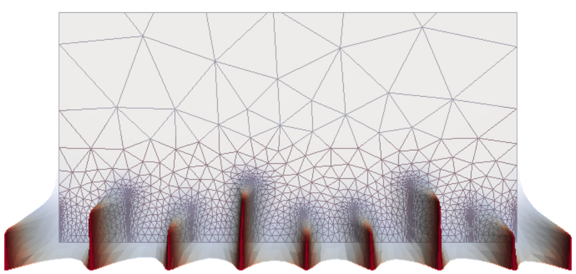

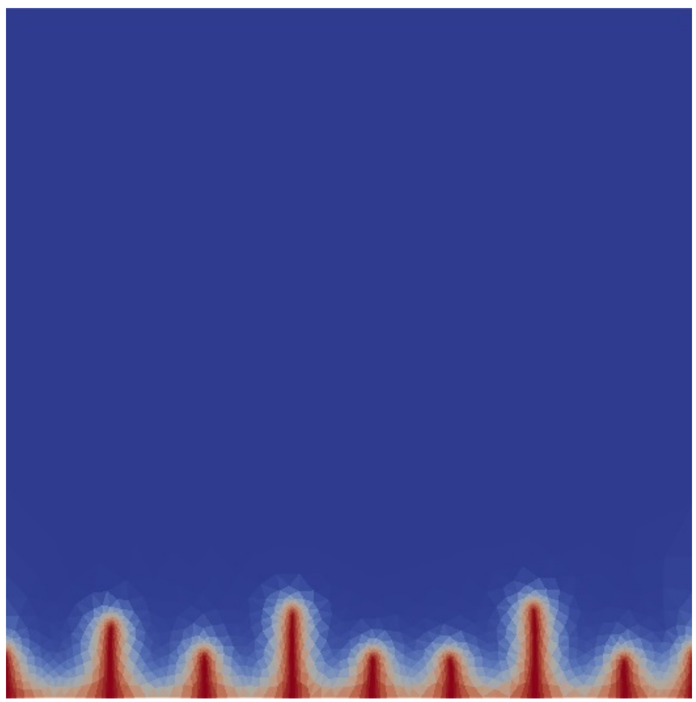

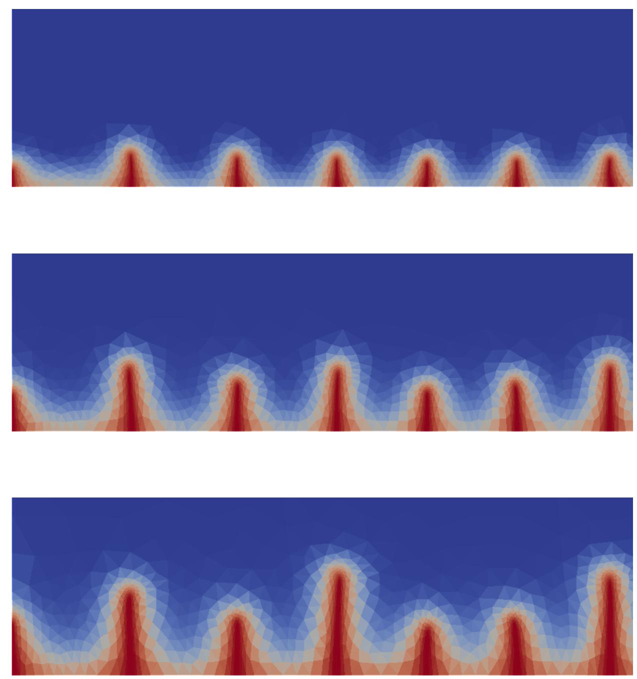

[N. Ferro, S.Micheletti, S.P., 2018]

Image segmentation

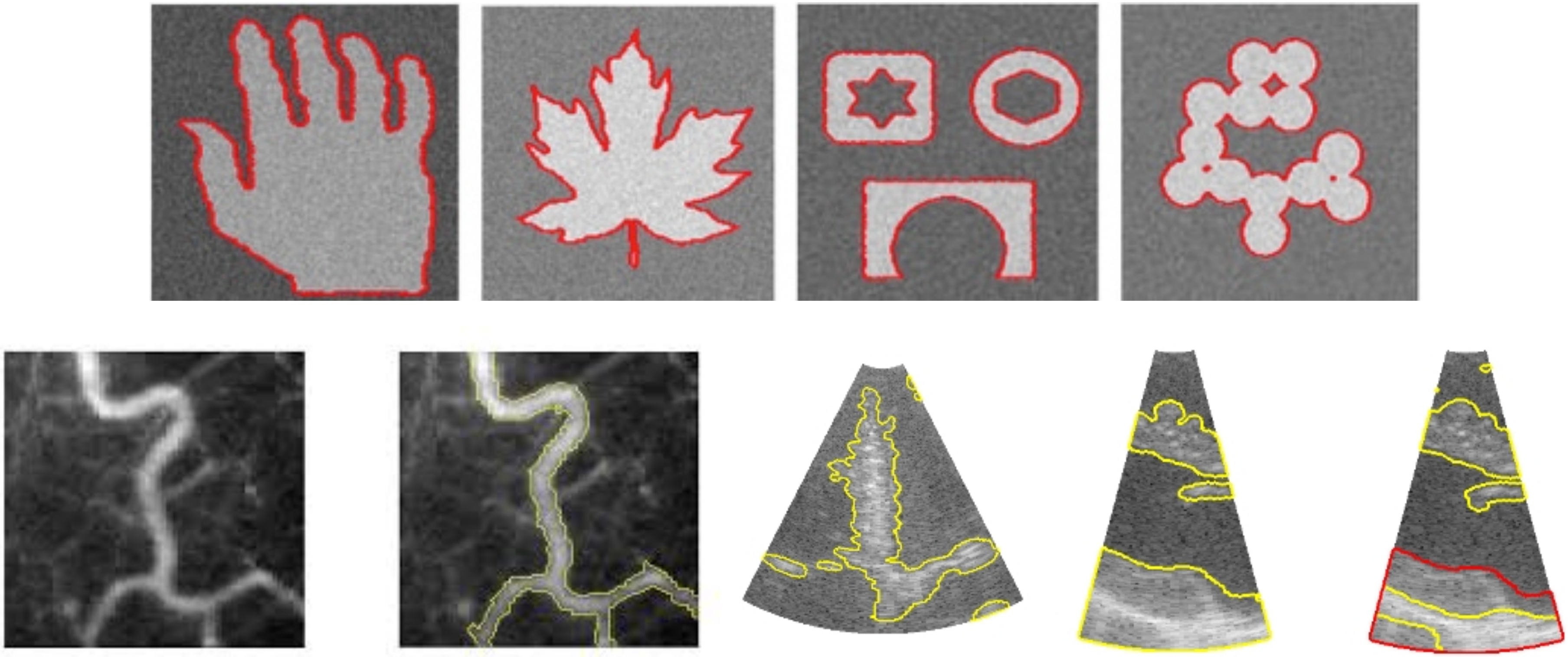

- thresholding/clustering/edge-detection/region-growing methods;
- PDE-based methods (e.g., level set method);
- variational methods.

Goal: identification of subregions of interest in a greyscale image.

Mesh adaptation-aided image segmentation

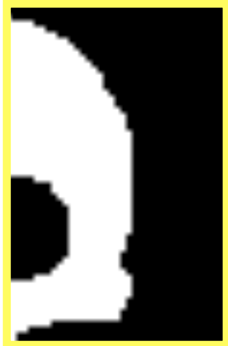

strong gradients across the image edges

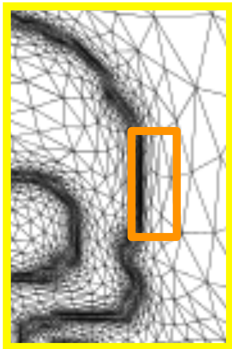

anisotropic adapted meshes sharply capture these features

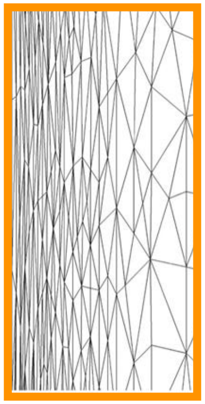

reduce the dofs (or increase the accuracy) by tuning size, shape and orientation of mesh elements

[e.g., M. Fortin, J. Dompierre, W.G. Habashi, M.G. Vallet et al. (2000,2002)]

Goal: identification of subregions of interest in a greyscale image.

Image segmentation: a variational model

[D. Mumford, J. Shah (1989); B. Bourdin (1999); A. Chambolle (1995)]

variational approximation

$$I(u,E) = \int_\Omega (u-f)^2\, d\Omega + \beta \int_{\Omega\setminus E} |\nabla u|^2\, d\Omega + \gamma\, \mathcal{H}(E)$$

(Mumford-Shah)

original image

separating edge

- $f \in L^\infty(\Omega)$
- E closed one-dimensional subset of Ω
- $u \in H^1(\Omega \setminus E)$
- β, γ positive parameters

Image segmentation: a variational model

[D. Mumford, J. Shah (1989);
B. Bourdin (1999); A. Chambolle (1995)]

$$I(u,E) = \underbrace{\int_{\Omega} (u-f)^2 \, d\Omega}_{\text{mismatch}} + \beta \underbrace{\int_{\Omega \setminus E} |\nabla u|^2 \, d\Omega}_{\text{smoothness}} + \underbrace{\gamma\, \mathcal{H}(E)}_{\text{Hausdorff measure}}$$

(Mumford-Shah)

- $f \in L^{\infty}(\Omega)$
- E closed one-dimensional subset of Ω
- $u \in H^1(\Omega \setminus E)$
- β, γ positive parameters

numerically hard

Ambrosio-Tortorelli approximation

$$I_\epsilon(u,v) = \boxed{\int_{\Omega} (u-f)^2 \, d\Omega} + \beta \int_{\Omega} (v^2+\eta)|\nabla u|^2 \, d\Omega + \gamma \int_{\Omega} \left(\epsilon |\nabla v|^2 + \frac{1}{4\epsilon}(v-1)^2 \right) d\Omega$$

- v with values in $[0, 1]$: approximate indicator of the set E with thickness ϵ

object boundary

object and background

[L. Ambrosio, V.M. Tortorelli (1990,1992)]
[P. D'Ambra, G. Tartaglione (2015)]

Image segmentation: a variational model

[D. Mumford, J. Shah (1989); B. Bourdin (1999); A. Chambolle (1995)]

$$I(u,E) = \underbrace{\int_\Omega (u-f)^2\, d\Omega}_{\text{mismatch}} + \beta \underbrace{\int_{\Omega\setminus E} |\nabla u|^2\, d\Omega}_{\text{smoothness}} + \gamma \underbrace{\mathcal{H}(E)}_{\text{Hausdorff measure}}$$

(Mumford-Shah)

- $f \in L^\infty(\Omega)$
- E closed one-dimensional subset of Ω
- $u \in H^1(\Omega \setminus E)$
- β, γ positive parameters

numerically hard

Ambrosio-Tortorelli approximation

$$I_\epsilon(u,v) = \int_\Omega (u-f)^2\, d\Omega + \beta \int_\Omega (v^2+\eta)|\nabla u|^2\, d\Omega + \gamma \int_\Omega \left(\epsilon|\nabla v|^2 + \frac{1}{4\epsilon}(v-1)^2\right) d\Omega$$

$\boxed{u \text{ and } v \text{ defined on the whole } \Omega}$

[L. Ambrosio, V.M. Tortorelli (1990,1992)]
[P. D'Ambra, G. Tartaglione (2015)]

Image segmentation: a variational model

[D. Mumford, J. Shah (1989); B. Bourdin (1999); A. Chambolle (1995)]

$$I(u,E) = \underbrace{\int_\Omega (u-f)^2\, d\Omega}_{\text{mismatch}} + \underbrace{\beta \int_{\Omega\setminus E} |\nabla u|^2\, d\Omega}_{\text{smoothness}} + \underbrace{\gamma\,\mathcal{H}(E)}_{\text{Hausdorff measure}}$$

(Mumford-Shah)

- $f \in L^\infty(\Omega)$
- E closed one-dimensional subset of Ω
- $u \in H^1(\Omega \setminus E)$
- β, γ positive parameters

numerically hard

Ambrosio-Tortorelli approximation

$$I_\epsilon(u,v) = \int_\Omega (u-f)^2\, d\Omega + \beta \int_\Omega (v^2+\eta)|\nabla u|^2\, d\Omega + \gamma \int_\Omega \left(\epsilon|\nabla v|^2 + \frac{1}{4\epsilon}(v-1)^2\right) d\Omega$$

$$\boxed{\{I_\epsilon\}_\epsilon \text{ is } \Gamma\text{- convergent to } I(u,E) \text{ for } \epsilon \to 0}$$

MOX

[L. Ambrosio, V.M. Tortorelli (1990,1992)]
[P. D'Ambra, G. Tartaglione (2015)]

Synthetic images

[A.S. Chiappa, S. Micheletti, R. Peli, S.P., submitted]

(sensitivity to model parameters)

sensitivity to ε

(a) true image

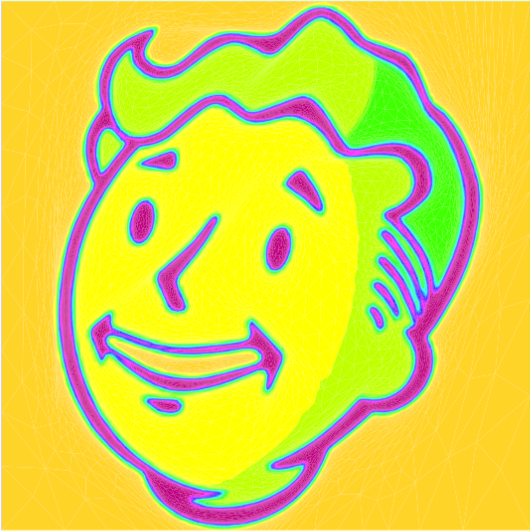

(b) approximate image u_h

16472 triangles

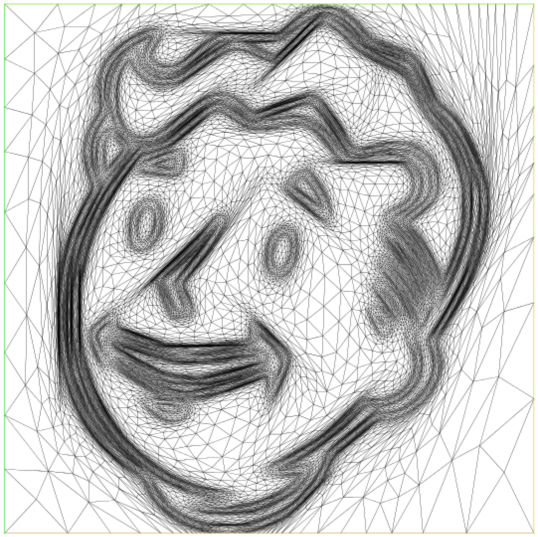

(c) anisotropic adapted mesh

(d) approximate indicator v_h

$$\epsilon = 5 \cdot 10^{-2}, \eta = 10^{-4}, \beta = 10^{-2}, \gamma = 4,$$

$$\mathtt{TOL} = 50, \mathtt{TOLs} = 10^{-2}, \mathtt{TOLfp} = 5 \cdot 10^{-3}, \mathtt{Ns} = 10, \mathtt{Nfp} = 30$$

Synthetic images

[A.S. Chiappa, S. Micheletti, R. Peli, S.P., submitted]

(sensitivity to model parameters)

sensitivity to ε

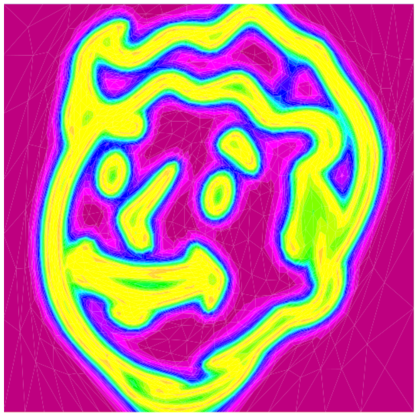

(a) $\epsilon = 1$: indicator v_h

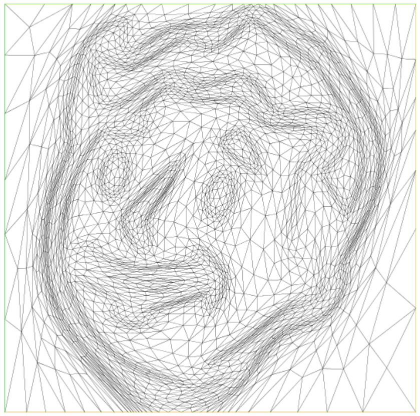

(b) $\epsilon = 1$: adapted mesh

(c) $\epsilon = 5 \cdot 10^{-1}$: indicator v_h

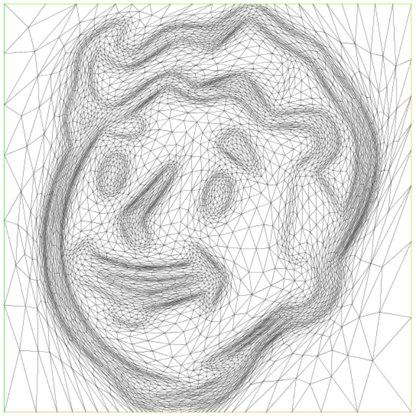

(d) $\epsilon = 5 \cdot 10^{-1}$: adapted mesh

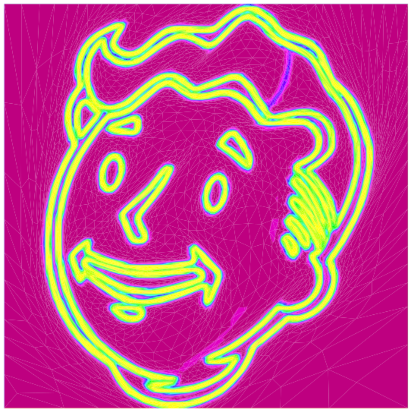

(e) $\epsilon = 10^{-1}$: indicator v_h

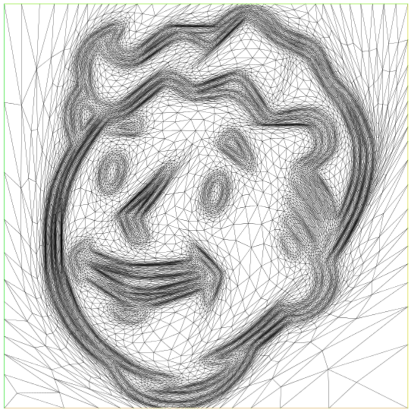

(f) $\epsilon = 10^{-1}$: adapted mesh

(g) $\epsilon = 5 \cdot 10^{-2}$: indicator v_h

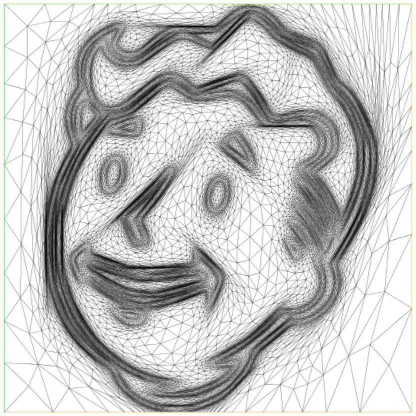

(h) $\epsilon = 5 \cdot 10^{-2}$: adapted mesh

ϵ	$\max_K s_K$	# vertices	# elements
1	38.71	2654	5236
$5 \cdot 10^{-1}$	34.43	4455	8834
10^{-1}	140.91	11426	22752
$5 \cdot 10^{-2}$	381.39	16472	32855

Synthetic images

[A.S. Chiappa, S. Micheletti, R. Peli, S.P., submitted]

(sensitivity to model parameters)

sensitivity to β

$$\epsilon = 10^{-1}, \eta = 10^{-4}, \ \ \gamma = 4,$$

$$\texttt{TOL} = 80, \texttt{TOLs} = 10^{-2},$$

$$\texttt{TOLfp} = 5 \cdot 10^{-3},$$

$$\texttt{Ns} = 10, \texttt{Nfp} = 50$$

β	$\max_K s_K$	# vertices	# elements
1.5	97.78	19560	39077
1	66.01	16572	33097
$5 \cdot 10^{-1}$	107.31	12294	24553

(b) $\beta = 1.5$: indicator v_h

(c) $\beta = 1.5$: adapted mesh

(d) $\beta = 1$: indicator v_h

(e) $\beta = 1$: adapted mesh

(f) $\beta = 5 \cdot 10^{-1}$: indicator v_h

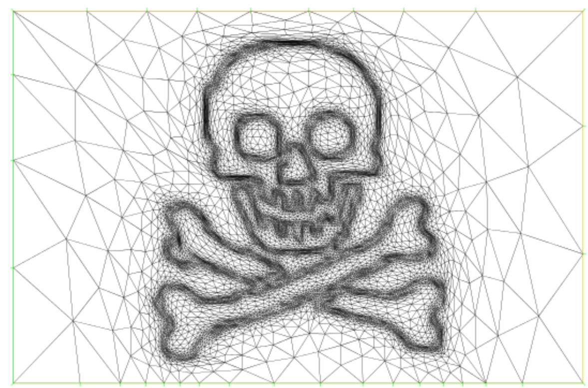

(g) $\beta = 5 \cdot 10^{-1}$: adapted mesh

Synthetic images

[A.S. Chiappa, S. Micheletti, R. Peli, S.P., submitted]

(sensitivity to model parameters)

sensitivity to γ

γ	$\max_K s_K$	# vertices	# elements
4	145.09	23455	46727
1	149.50	16246	32299
0.25	218.44	11109	22033

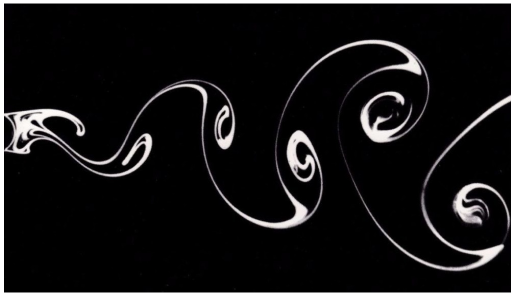

(a) true image

$\epsilon = 10^{-1}$, $\eta = 10^{-4}$,

$\beta = 5 \cdot 10^{-2}$, $\mathtt{TOL} = 80$,

$\mathtt{TOLs} = 10^{-2}$,

$\mathtt{TOLfp} = 5 \cdot 10^{-3}$,

$\mathtt{Ns} = 10$, $\mathtt{Nfp} = 50$

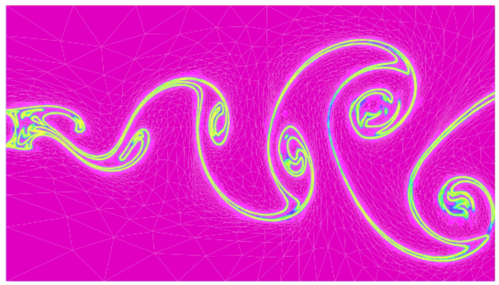

(b) $\gamma = 4$: indicator v_h

(c) $\gamma = 4$: thresholded indicator

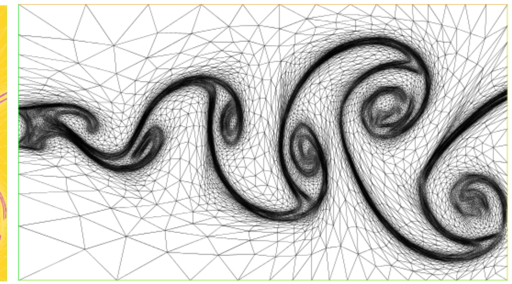

(d) $\gamma = 4$: adapted mesh

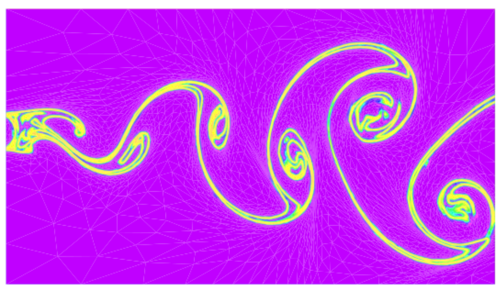

(e) $\gamma = 1$: indicator v_h

(f) $\gamma = 1$: thresholded indicator

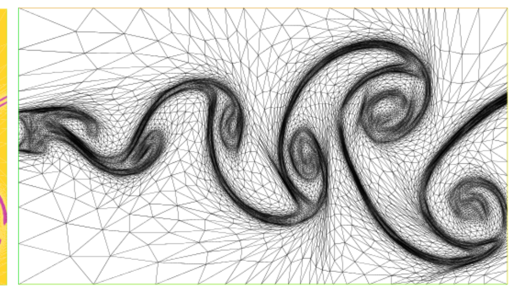

(g) $\gamma = 1$: adapted mesh

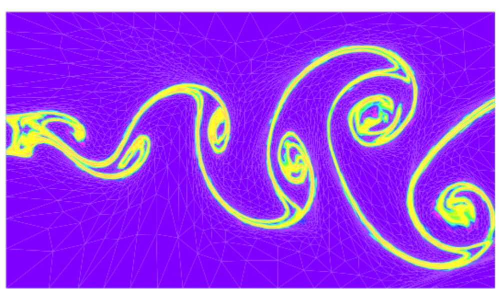

(h) $\gamma = 0.25$: indicator v_h

(i) $\gamma = 0.25$: thresholded indicator

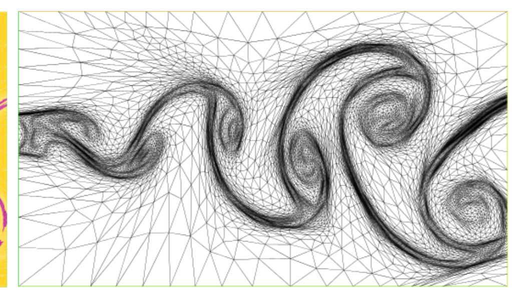

(j) $\gamma = 0.25$: adapted mesh

Real images

[A.S. Chiappa, S. Micheletti, R. Peli, S.P., submitted]

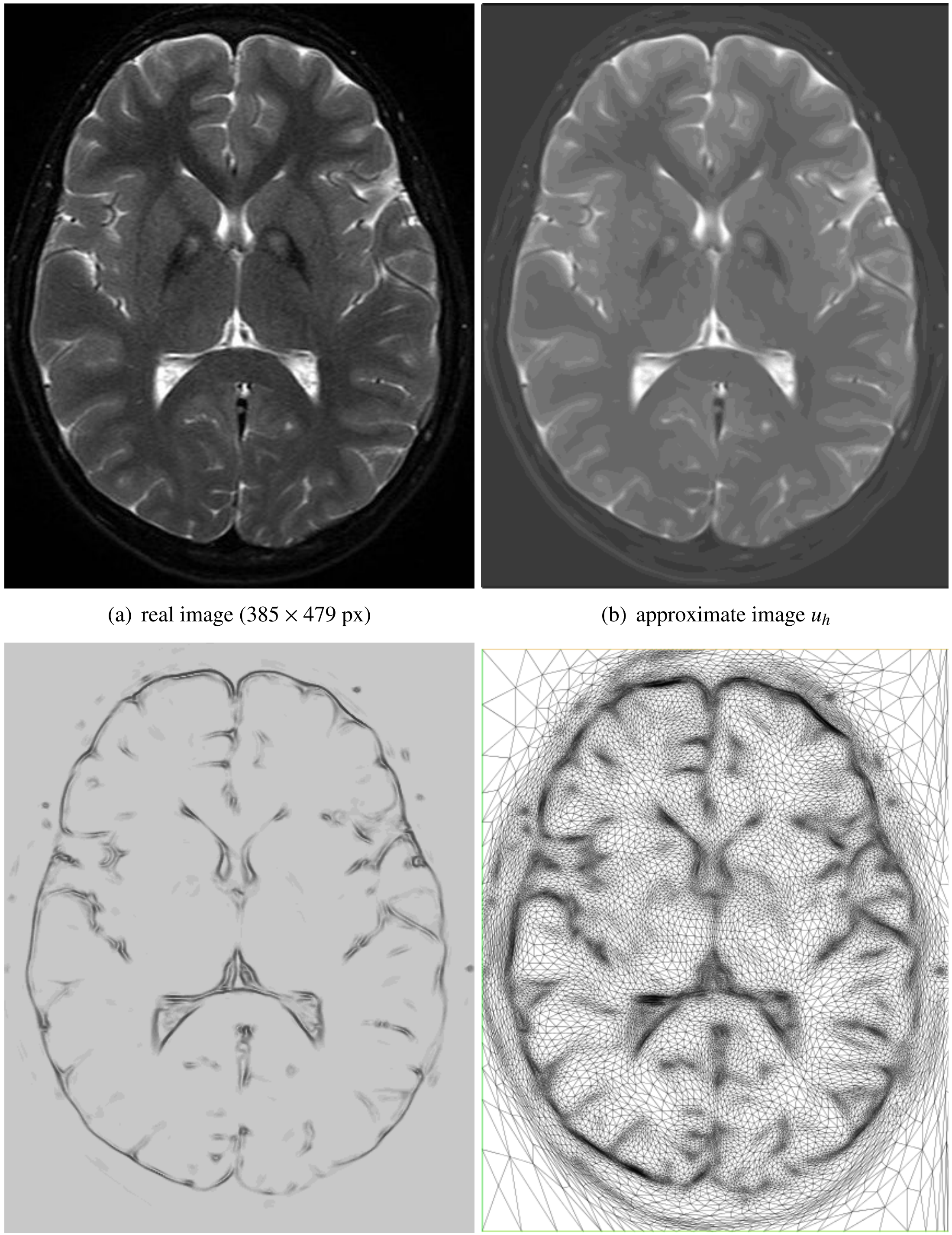

(a) real image (385 × 479 px) (b) approximate image u_h

(c) indicator v_h (d) adapted mesh

39334 triangles

https://it.m.wikipedia.org/wiki/File:Pkan-basal-ganglia-MRI.JPG

Real images

[A.S. Chiappa, S. Micheletti, R. Peli, S.P., submitted]

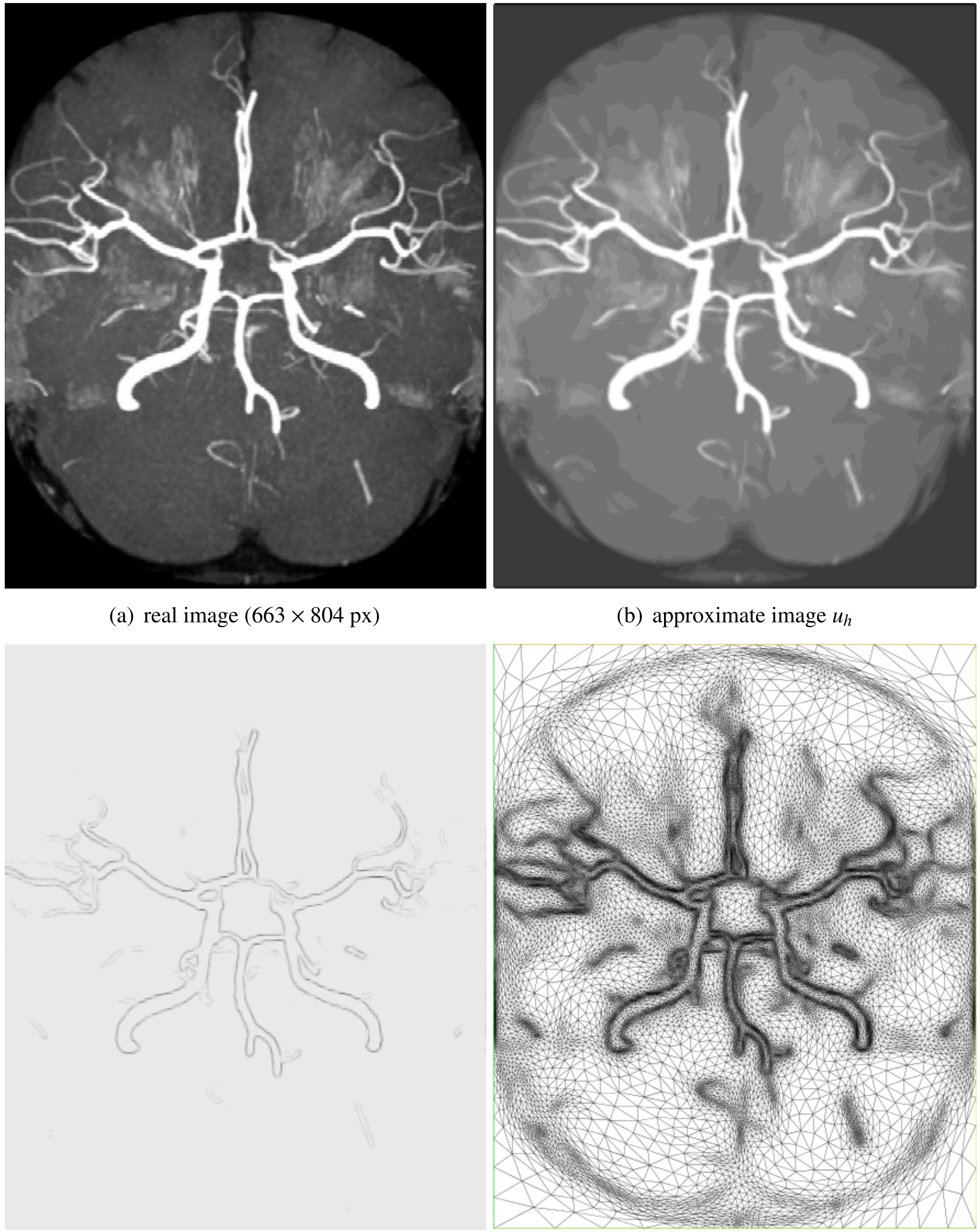

(a) real image (663 × 804 px) (b) approximate image u_h

(c) indicator v_h (d) adapted mesh

49544 triangles

https://www.spandidos-publications.com/br/3/1/55

Real images

[A.S. Chiappa, S. Micheletti, R. Peli, S.P., submitted]

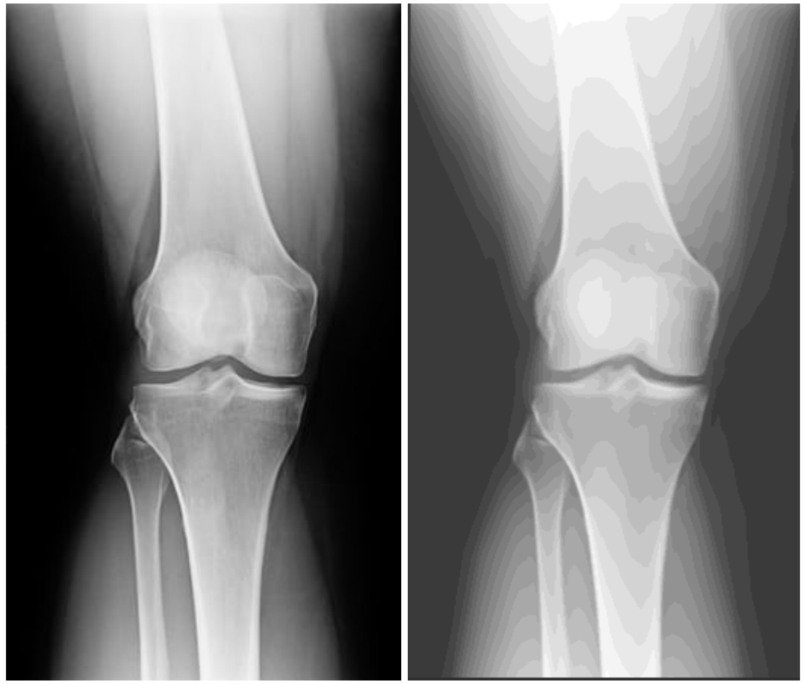

(a) real image (261 × 448 px) (b) approximate image u_h

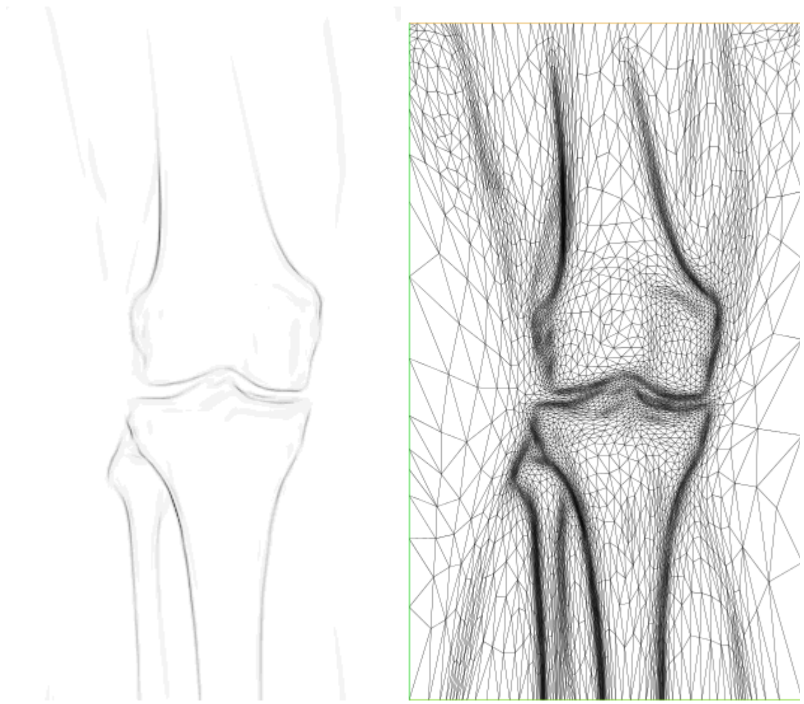

(c) indicator v_h (d) adapted mesh

11175 triangles

https://www.howardluksmd.com/orthopedic-social-media/medial-joint-space-narrowing/

Real images

[A.S. Chiappa, S. Micheletti, R. Peli, S.P., submitted]

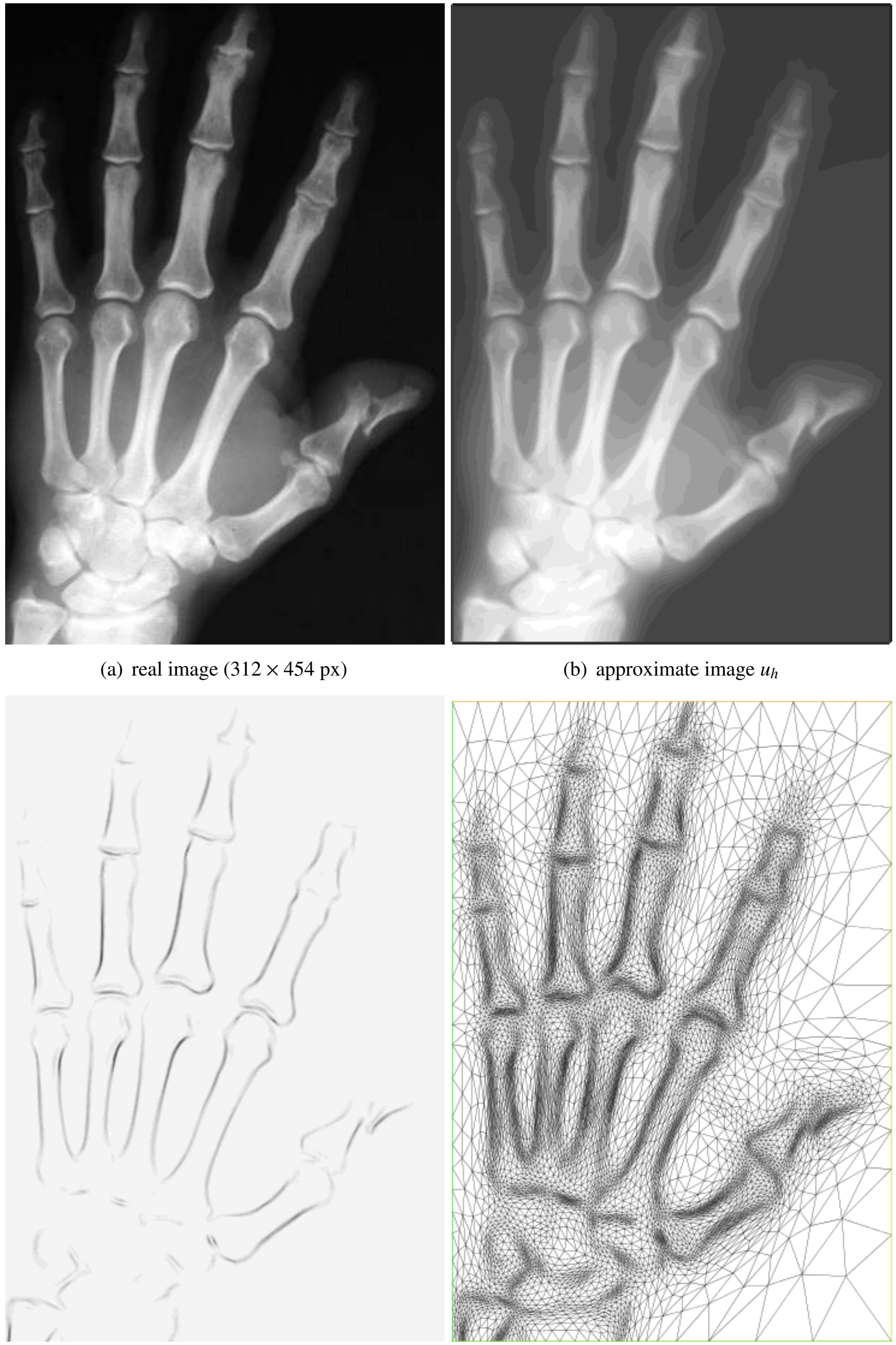

(a) real image (312 × 454 px) (b) approximate image u_h

(c) indicator v_h (d) adapted mesh

17056 triangles

https://it.wikipedia.org/wiki/File:Artrite_psoriasica_Rx_Mano_Sn.PNG

Real images

[A.S. Chiappa, S. Micheletti, R. Peli, S.P., submitted]

input parameters

image	ϵ	β	γ	η	TOL	TOLs	TOLfp	Ns	Nfp
brain	10^{-3}	10^{-1}	$5 \cdot 10^{-1}$	10^{-6}	70	10^{-2}	$5 \cdot 10^{-3}$	10	40
Willis	10^{-3}	10^{-1}	5	10^{-6}	100	10^{-2}	$5 \cdot 10^{-3}$	10	40
knee	10^{-3}	$2 \cdot 10^{-1}$	10	10^{-6}	60	10^{-2}	$5 \cdot 10^{-3}$	10	40
hand	10^{-3}	10^{-1}	10	10^{-6}	60	10^{-2}	$5 \cdot 10^{-3}$	10	40

output data

image	$\max_K s_K$	# vertices	# elements	# ITs	# ITfp
brain	71.94	19726	39334	4	4 – 8 – 9 – 25
Willis	56.51	24845	49544	3	2 – 4 – 4
knee	82.01	5683	11175	4	3 – 5 – 7 – 6
hand	38.01	8592	17056	5	2 – 3 – 2 – 2 – 2

output data

image	E-time	AD-time	FP-time
brain	170.74	43.77 – 24.95 – 19.45 – 17.58	11.26 – 12.57 – 10.62 – 25.51
Willis	102.78	29.76 – 24.12 – 22.93	3.63 – 5.78 – 5.3
knee	56.29	23.56 – 7.66 – 5.56 – 4.64	4.87 – 2.31 – 2.24 – 1.54
hand	79.90	29.83 – 11.32 – 8.53 – 7.48 – 7.3	4.14 – 2.01 – 0.97 – 0.87 – 0.81

Comparison with a pixel mesh

[B. Bourdin (1999)]

$$\epsilon = 10^{-1},\ \eta = 10^{-2},$$

$$\beta = 2,\ \gamma = 10^{-2}$$

$$\mathtt{TOL} = 50,\ \mathtt{TOLs} = 10^{-2},$$

$$\mathtt{TOLfp} = 5 \cdot 10^{-3},$$

$$\mathtt{Ns} = 10,\ \mathtt{Nfp} = 50$$

(a) real image (512×512 px)

(b) approximate image u_h

(c) thresholded indicator v_h

(d) adapted mesh

67679 triangles

[A.S. Chiappa, S. Micheletti, R. Peli, S.P., submitted]

Comparison with isotropic mesh adaptation

32855 triangles

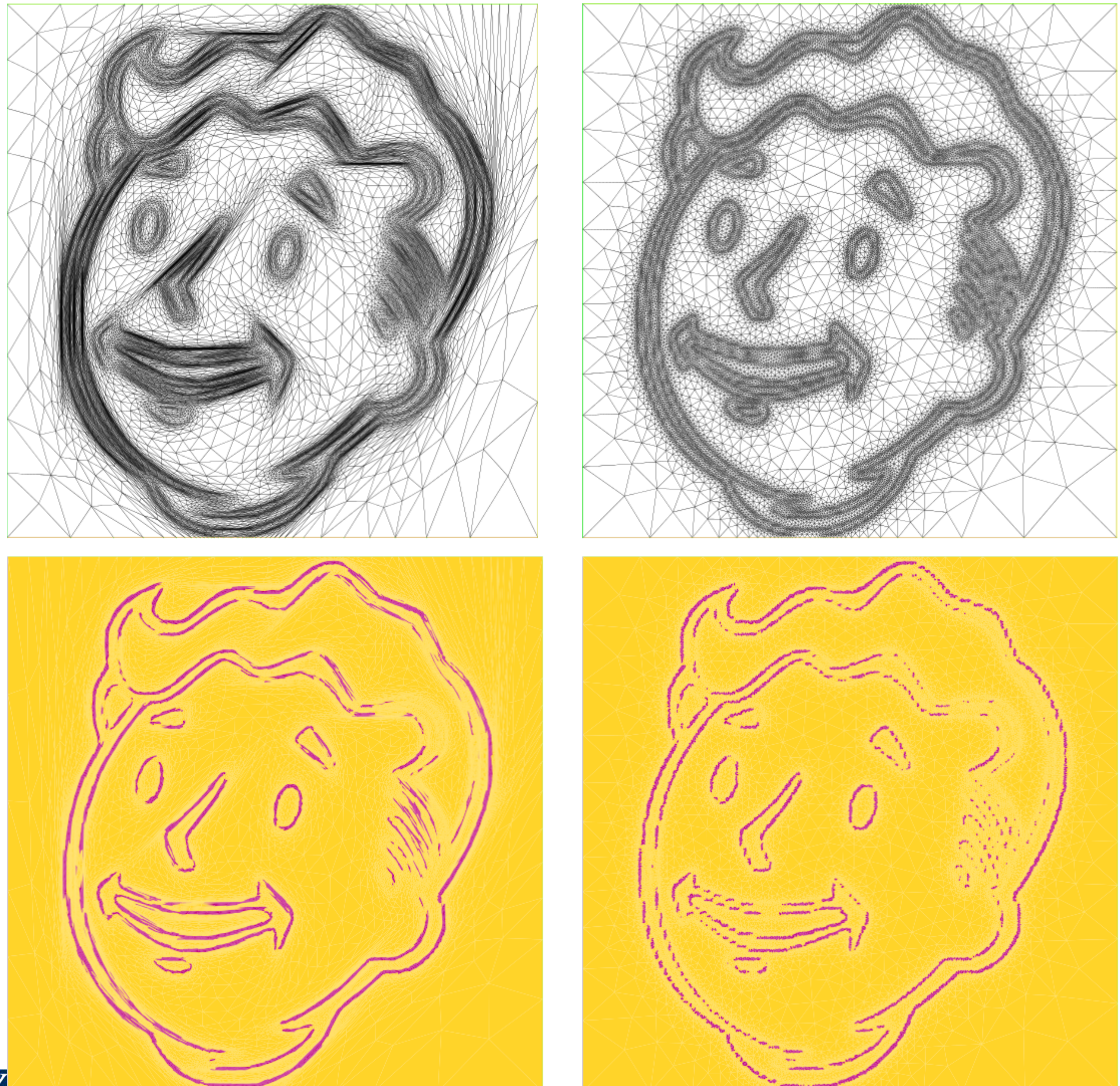

62023 triangles

[A.S. Chiappa, S. Micheletti, R. Peli, S.P., submitted]

Comparison with isotropic mesh adaptation

$\mathrm{TOL} = 70$

39334 triangles

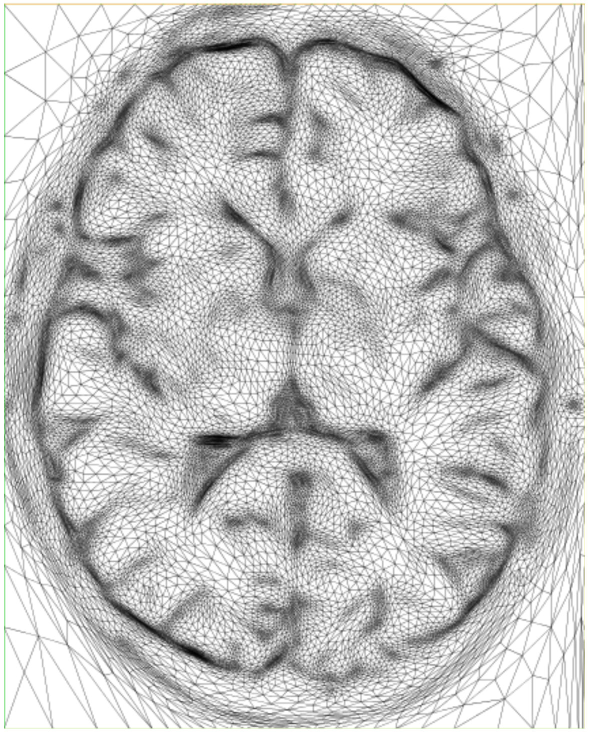

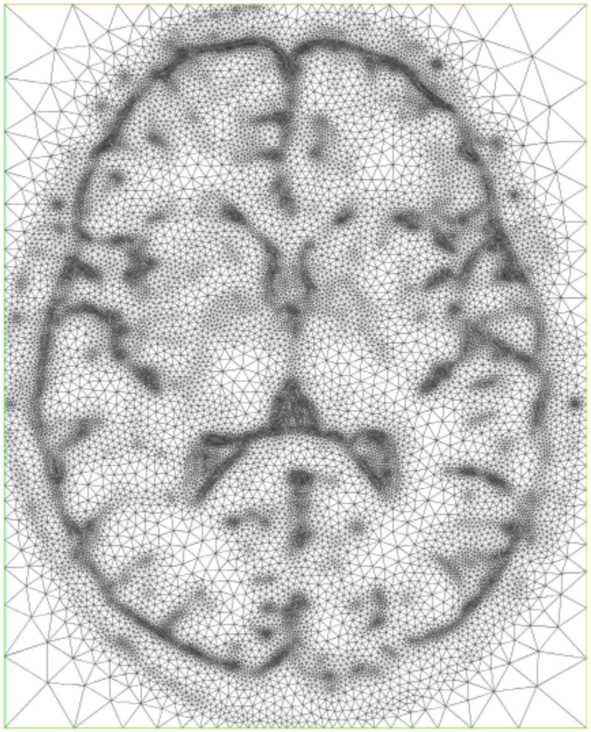

48829 triangles

$\mathrm{TOL} = 60$

11175 triangles

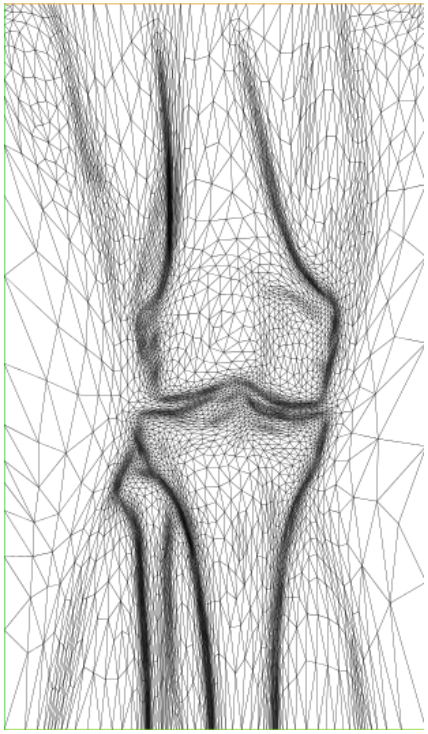

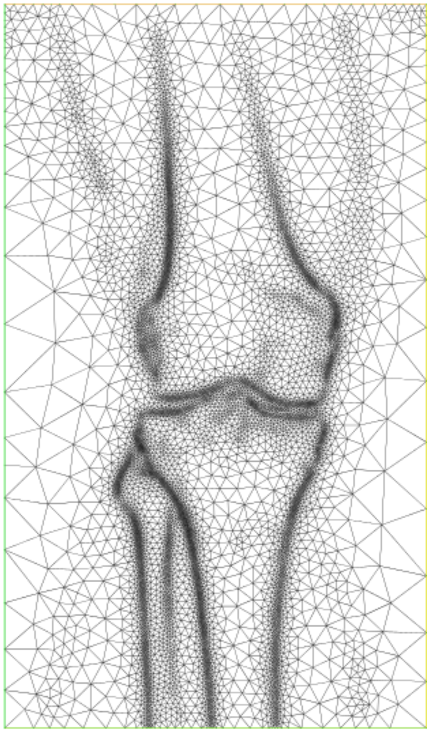

19760 triangles

[A.S. Chiappa, S. Micheletti, R. Peli, S.P., submitted]